Available online at http://scik.org
Commun. Math. Biol. Neurosci. 2025, 2025:72
https://doi.org/10.28919/cmbn/9097
ISSN: 2052-2541

MODELING THE IMPACT OF FOOD INSECURITY ON THE TRANSMISSION DYNAMICS OF MONKEYPOX USING THREE DIFFERENT FRACTIONAL OPERATORS

ROSE VERONICA PAUL[1], OBIORA CORNELIUS COLLINS[2], WILLIAM ATOKOLO[1,*]

[1]Department of Mathematical Sciences, Prince Abubakar Audu University, Anyigba 272102, Nigeria

[2]Institute of Systems Science, Durban University of Technology, Durban 4000, South Africa

Abstract. The global emergence of Monkeypox presents significant public health challenges, particularly in regions with varying levels of food insecurity. This study develops and analyzes a novel mathematical model examining the dynamics of Monkeypox transmission across food-secure and food-insecure human populations, while incorporating animal reservoirs. We investigate the system through three distinct arbitrary-order derivative operators: the Caputo derivative with power law, the Caputo-Fabrizio derivative with non-singular kernel, and the Atangana-Baleanu derivative incorporating the Mittag-Leffler function. The model explicitly considers the impact of food insecurity status on disease transmission rates, recovery patterns, and intervention effectiveness. Through numerical simulations, we demonstrate that food-insecure populations experience significantly higher infection peaks (approximately 12.5 million cases) compared to food-secure populations (approximately 9.5 million cases). Our analysis reveals how varying fractional orders ($\theta = 0.95$, 0.85, and 0.75) influence the temporal effects and overall disease dynamics. The model parameters, estimated from current epidemiological data and literature, provide insights into the critical role of food insecurity in disease mitigation. Surface plots analyzing the basic reproduction number R_0 against various parameters demonstrate the sensitivity of disease spread to contact rates, recovery rates, and food insecurity status. These findings emphasize the importance of integrating food security measures into public health interventions for effective Monkeypox control, particularly in vulnerable populations.

*Corresponding author

E-mail address: williamsatokolo@gmail.com

Received December 28, 2024

Keywords: Monkeypox; food insecurity; numerical analysis; Adams Bashforth Moulton method; fixed point theory.

2020 AMS Subject Classification: 00A71

1. INTRODUCTION

Monkeypox is a zoonotic viral disease first discovered in 1958, with the first human case reported in 1970 in the Democratic Republic of Congo [1, 2]. The disease is caused by the Monkeypox virus, a member of the Orthopoxvirus genus in the Poxviridae family, which is closely related to smallpox but clinically less severe [3, 4]. The primary signs and symptoms of Monkeypox include fever, headache, muscle aches, swollen lymph nodes, and a characteristic progressive skin rash that develops into fluid-filled and later scabbing lesions [5, 6]. It can be transmitted through proximity with infected persons, bodily fluids, contaminated materials, and potentially through respiratory droplets [7, 8]. Treatment for Monkeypox is basically auxiliary in nature, Concentrating on symptom management, preventing secondary infections, and providing hydration and nutritional support [9, 10]. Antiviral medications like tecovirimat, originally developed for smallpox, have shown potential efficacy in managing severe cases [11, 12]. Globally, the 2022 Monkeypox outbreak represented a significant public health event, with the World Health Organization reporting over 87,000 cases across 110 countries by January 2023, marking an unprecedented spread beyond traditional endemic regions in Africa [13, 14, 15].

Food is one of the most critical items in the world, essential to human survival alongside clothing and shelter. Food insecurity, defined as the inability to consistently access safe, nutritious, and affordable food, poses a significant challenge to global health and well-being [16]. In the wake of global food crisis of 1970's, The idea of food security was popularized by Food and Agricultural Organization (FAO), an organ of the United Nations, aiming to address hunger by ensuring sufficient food production, reliable supply chains, and protection from price fluctuations [17]. Food insecurity can manifest in two forms: chronic, characterized by prolonged inadequate access to nutritious food, and transitory, reflecting temporary food shortages in a community. The drivers of food insecurity include adverse climatic conditions, political and economic instability, escalating food costs, violence, terrorism, weak agricultural systems, high unemployment, and inflation. Its impacts, such as hunger, malnutrition, weakened immunity,

and poverty, are particularly severe in Africa, the region with the highest rates of food insecurity globally. In Nigeria, for example, over 31.8 million people face acute food insecurity exacerbated by rising food prices and security challenges (FAO). Due to these conditions, individuals often resort to consuming contaminated or infected animal products to meet daily caloric needs, increasing the risk of zoonotic disease outbreaks like Monkeypox [18, 19].

Fractional calculus represents a sophisticated mathematical framework extending beyond traditional integer-order derivatives, enabling more nuanced modeling of complex systems. [25] have demonstrated its profound potential in translating abstract mathematical concepts into practical solutions across diverse scientific domains [24]. The versatility of arbitrary-order derivatives spans multiple disciplines, including advanced signal processing, complex biomathematical systems, epidemiological modeling, and sophisticated public health interventions [20, 21, 22]. Contemporary research has predominantly categorized these derivatives into two fundamental classes: singular and non-singular mathematical representations. Pioneering work by Podlubny on Riemann-Liouville and Caputo operators has established foundational approaches for power law kernel-based mathematical transformations [26]. Recent investigations have critically examined these traditional kernel structures, proposing innovative non-singular modifications that enhance computational flexibility and predictive accuracy. Emerging fractional modeling techniques have introduced sophisticated derivative approaches, such as the Caputo-Fabrizio derivative utilizing exponential law kernels and the Atangana-Baleanu derivative leveraging Mittag-Leffler kernel representations with remarkable non-local characteristics [33, 27].

Researchers have increasingly focused on modeling infectious disease transmission using difference approach, as demonstrated in numerous studies. [1] employ two modeling methods to examine the spread and efficient control measures for Mpox virus. [30] developed mathematical models using Laplace Adomian Decomposition approaches, analyzing stability through advanced mathematical techniques. [29] investigated disease dynamics using fractional derivative approaches, providing comprehensive analytical and numerical solutions. [31] utilizes a new numerical approach that pertains to non-singular kernels to investigate the spread and management of Monkey pox virus.

The novelty of this research lies in investigating the effect of fractional order on Monkeypox transmission dynamics, with a specific focus on the impact of food insecurity as a critical control measure. By examining the disease system within the structure of fractional derivative operators using three distinct kernel types, we aim to provide a more nuanced understanding of disease transmission mechanisms. The advantages of the proposed approach using fractional operators are significant. Fractional-order derivatives can approximate real-world data with greater flexibility than classical derivatives, accounting for non-locality and exhibiting remarkable memory effects. These characteristics allow for a more sophisticated representation of complex disease transmission systems that traditional models cannot capture. To ensure robust model development, we implemented cross-validation techniques, temporal and spatial validation, and parameter simplification strategies. These methodological considerations address potential limitations of fractional-order models, such as the risk of over-fitting, and enhance the model's generalizability and predictive capabilities.

This work is structured as follows: Section (1.1) introduces the mathematical foundations for fractional-order derivatives. Section (2) outlines the formulation of the mathematical model in both classical and fractional-order frameworks. In Section (3), numerical methods are detailed for the fractional Caputo derivative with a power-law kernel and the Caputo-Fabrizio derivative with an exponential kernel. This section also includes an investigation into the existence and uniqueness of solutions, alongside the corresponding numerical schemes. Section (4) focuses on the analysis of the Mpox model using the Atangana-Baleanu (AB) derivative operator and presents the results of the model simulations. Finally, Section (6) summarizes the conclusions and numerical findings derived from the study.

1.1. Fractional Calculus Preliminaries. This section provides essential definitions and results foundational to this study. Key definitions related to the various kernels necessary for the research are succinctly outlined [35, 36, 37, 38, 39, 40].

Definition 1.1. [26]. *The Liouville-Caputo fractional order derivative of order* $\theta \in [0,1)$ *is defined as:*

$$ {}_0^C D_t^{\theta} x(t) = \frac{1}{\Gamma(1-\theta)} \int_0^t (t-\psi)^{-\theta} \frac{d}{dt} x(\psi)\, d\psi. \tag{1} $$

Definition 1.2. [33] *The Caputo-Fabrizio (CF) derivative, which features a nonsingular kernel, of a function $x(t)$ with fractional order $\theta \in (0,1)$ is defined as:*

$$ {}_{0}^{CF}D_{t}^{\theta}x(t) = \frac{N(\theta)}{1-\theta}\int_{0}^{t}\exp\left[-\frac{\theta(t-\psi)}{1-\theta}\right]\frac{d}{dt}x(\psi)\,d\psi, \tag{2} $$

Where $N(\theta) = N(0) = N(1)$. Secondly,

$x \in Q^{'}(0,T), T > 0.$

Definition 1.3. [41] *The fractional order integral of a function $x(t)$ with order $\theta \in (0,1)$ is defined as:*

$$ {}_{0}^{CF}I_{t}^{\theta}x(t) = \frac{2(1-\theta)}{(2-\theta)N(\theta)}x(t) + \frac{2\theta}{(2-\theta)N(\theta)}\int_{0}^{t}x(\psi)\,d\psi. \tag{3} $$

Definition 1.4. [32] *The Atangana-Baleanu (AB) fractional order operator in the Caputo sense, with order $\theta \in (0,1)$, is defined as:*

$$ {}_{0}^{ABC}D_{t}^{\theta}x(t) = \frac{AB(\theta)}{(1-\theta)}\int_{0}^{t}\gamma_{0}\left[-\frac{\theta(t-\psi)^{\theta}}{1-\theta}\right]\frac{d}{dt}x(\psi)\,d\psi, \tag{4} $$

Where γ_{θ} is a Mittag-Leffler function and is defined as:

$$ \gamma_{\theta}(m) = \sum_{k=0}^{\infty}\frac{m^{k}}{\left|(\theta k+1)\right.}, \theta \in C, R(\theta) > 0, m \in C, $$

also $AB(\theta) = 1-\theta+\frac{\theta}{\left|(\theta)\right.}$ represents the normalization function.

The discussion of the fractional order integral associated with the Atangana-Baleanu derivative is defined as:

$$ {}_{0}^{AB}I_{t}^{\theta}x(t) = \frac{(1-\theta)}{AB(\theta)}x(t) + \frac{\theta}{AB(\theta)\left|(\theta)\right.}\int_{0}^{t}(t-\psi)^{\theta-1}x(\psi)\,d\psi \tag{5} $$

2. Mathematical Model Formulation

The monkeypox model is formulated by dividing the human population into six different compartments and the animal population is sub-divided into three compartments: susceptible individuals with food security (S_{FS}), infected individuals with food security (I_{FS}), recovered individuals with food security (R_{FS}), susceptible individuals with food insecurity (S_{FI}), infected

individuals with food insecurity (I_{FI}), recovered individuals with food insecurity (R_{FI}), susceptible animals (S_A), infected animals (I_A), and recovered animals (R_A). The following equations describe the dynamics of each compartment.

Susceptible Individuals with Food Security (S_{FS})**:** The susceptible individuals with food security are recruited at a rate $a\Lambda_S$, where Λ_S represents the birth rate and immigration into the human population, and the parameter a represents the fraction of the recruited individuals entering the food-secure population. This class decreases as susceptible individuals come into contact with infected individuals from the food-secure population (I_{FS}), food-insecure population (I_{FI}), and infected animals (I_A) at rates α_1, α_2, and α_3, respectively. These contacts triggers the spread of the disease. Additionally, susceptible individuals die due to natural mortality at a rate μ_H. The dynamics of susceptible individuals with food security is therefore given by:

$$\frac{dS_{FS}}{dt} = a\Lambda_S - \frac{m(\alpha_1 I_{FS} + \alpha_2 I_{FI} + \alpha_3 I_A)}{N_{FS}} S_{FS} - \mu_H S_{FS}.$$

Infected Individuals with Food Security (I_{FS})**:** The number of infected individuals with food security increases due to contacts with susceptible individuals from the food-secure and food-insecure populations, as well as infected animals, at rates α_1, α_2, and α_3, respectively. We define the parameter m as the modification parameter that accounts for the reduced rate of disease contraction in the food-secure population compared to the food-insecure populations. The infected population decreases due to recovery at rate τ_S, disease-induced mortality at rate δ_S, and natural mortality at rate μ_H. The equation for the infected individuals with food security is:

$$\frac{dI_{FS}}{dt} = \frac{m(\alpha_1 I_{FS} + \alpha_2 I_{FI} + \alpha_3 I_A)}{N_{FS}} S_{FS} - (\tau_S + \delta_S + \mu_H) I_{FS}.$$

Recovered Individuals with Food Security (R_{FS})**:** Recovered individuals with food security are those who have recovered from infection. The number of individuals in this compartment increases due to recovery from the infected food-secure individuals at a rate τ_S and decreases due to natural mortality at a rate μ_H. The equation for recovered individuals with food security is:

$$\frac{dR_{FS}}{dt} = \tau_S I_{FS} - \mu_H R_{FS}.$$

Susceptible Individuals with Food Insecurity (S_{FI})**:** The susceptible individuals with food insecurity are recruited at a rate $(1-a)\Lambda_S$, where $(1-a)$ represents the fraction of the recruited individuals entering the food-insecure population. This class decreases as susceptible individuals come into contact with infected individuals from the food-secure and food-insecure populations and infected animals, at rates α_4, α_5, and α_6, respectively. Additionally, susceptible individuals die due to natural mortality at a rate μ_H. The dynamics of susceptible individuals with food insecurity is:

$$\frac{dS_{FI}}{dt} = (1-a)\Lambda_S - \frac{(\alpha_4 I_{FS} + \alpha_5 I_{FI} + \alpha_6 I_A)}{N_{FI}} S_{FI} - \mu_H S_{FI}.$$

Infected Individuals with Food Insecurity (I_{FI})**:** The infected individuals with food insecurity increase due to contacts with susceptible individuals from the food-secure and food-insecure populations, as well as infected animals, at rates α_4, α_5, and α_6, respectively. The infected population decreases due to recovery at rate τ_I, disease-induced mortality at rate δ_I, and natural mortality at rate μ_H. The equation for infected individuals with food insecurity is:

$$\frac{dI_{FI}}{dt} = \frac{(\alpha_4 I_{FS} + \alpha_5 I_{FI} + \alpha_6 I_A)}{N_{FI}} S_{FI} - (\tau_I + \delta_I + \mu_H) I_{FI}.$$

Recovered Individuals with Food Insecurity (R_{FI})**:** Recovered individuals with food insecurity are those who have recovered from infection. The number of individuals in this compartment increases due to recovery from the infected food-insecure individuals at a rate τ_I and decreases due to natural mortality at a rate μ_H. The equation for recovered individuals with food insecurity is:

$$\frac{dR_{FI}}{dt} = \tau_I I_{FI} - \mu_H R_{FI}.$$

Susceptible Animals (S_A)**:** Susceptible animals are recruited at a rate Λ_A, and they decrease as they come into contact with infected animals at a rate α_7. Additionally, animals die due to natural mortality at rate μ_A. The equation for susceptible animals is:

$$\frac{dS_A}{dt} = \Lambda_A - \frac{\alpha_7 I_A}{N_A} S_A - \mu_A S_A.$$

Infected Animals (I_A)**:** Infected animals increase due to contact with susceptible animals at rate α_7. The infected animal population decreases due to recovery at rate τ_A, disease-induced mortality at rate δ_A, and natural mortality at rate μ_A. The equation for infected animals is:

$$\frac{dI_A}{dt} = \frac{\alpha_7 I_A}{N_A} S_A - (\tau_A + \delta_A + \mu_A) I_A.$$

Recovered Animals (R_A)**:** Recovered animals are those that have recovered from infection. The number of individuals in this compartment increases due to recovery from infected animals at a rate τ_A and decreases due to natural mortality at a rate μ_A. The equation for recovered animals is:

$$\frac{dR_A}{dt} = \tau_A I_A - \mu_A R_A.$$

The sum of food-secure humans is given as:

$$N_{FS} = S_{FS} + I_{FS} + R_{FS}$$

The sum of food-insecure humans is given as:

$$N_{FS} = S_{FI} + I_{FI} + R_{FI}$$

The sum of animal population is given as:

$$N_A = S_A + I_A + R_A$$

The mathematical model based on our assumptions and the described framework is presented as follows:

$$\begin{aligned}
\frac{dS_{FS}}{dt} &= a\Lambda_S - \frac{m(\alpha_1 I_{FS} + \alpha_2 I_{FI} + \alpha_3 I_A)}{N_{FS}} S_{FS} - \mu_H S_{FS} \\
\frac{dI_{FS}}{dt} &= \frac{m(\alpha_1 I_{FS} + \alpha_2 I_{FI} + \alpha_3 I_A)}{N_{FS}} S_{FS} - (\tau_S + \delta_S + \mu_H) I_{FS} \\
\frac{dR_{FS}}{dt} &= \tau_S I_{FS} - \mu_H R_{FS} \\
\frac{dSFI}{dt} &= (1-a)\Lambda_S - \frac{(\alpha_4 I_{FS} + \alpha_5 I_{FI} + \alpha_6 I_A)}{N_{FI}} S_{FI} - \mu_H S_{FI} \\
\frac{dI_{FS}}{dt} &= \frac{\alpha_4 I_{FS} + \alpha_5 I_{FI} + \alpha_6 I_A}{N_{FI}} S_{FI} - (\tau_I + \delta_I + \mu_H) I_{FS} \\
\frac{dR_{FI}}{dt} &= \tau_I I_{FI} - \mu_H R_{FI} \\
\frac{dS_A}{dt} &= \Lambda_A - \frac{\alpha_7 I_A}{N_A} S_A - \mu_A S_A \\
\frac{dI_A}{dt} &= \frac{\alpha_7 I_A}{N_A} S_A - (\tau_A + \delta_A + \mu_A) I_A \\
\frac{dRA}{dt} &= \tau_A I_A - \mu_A R_A
\end{aligned} \tag{6}$$

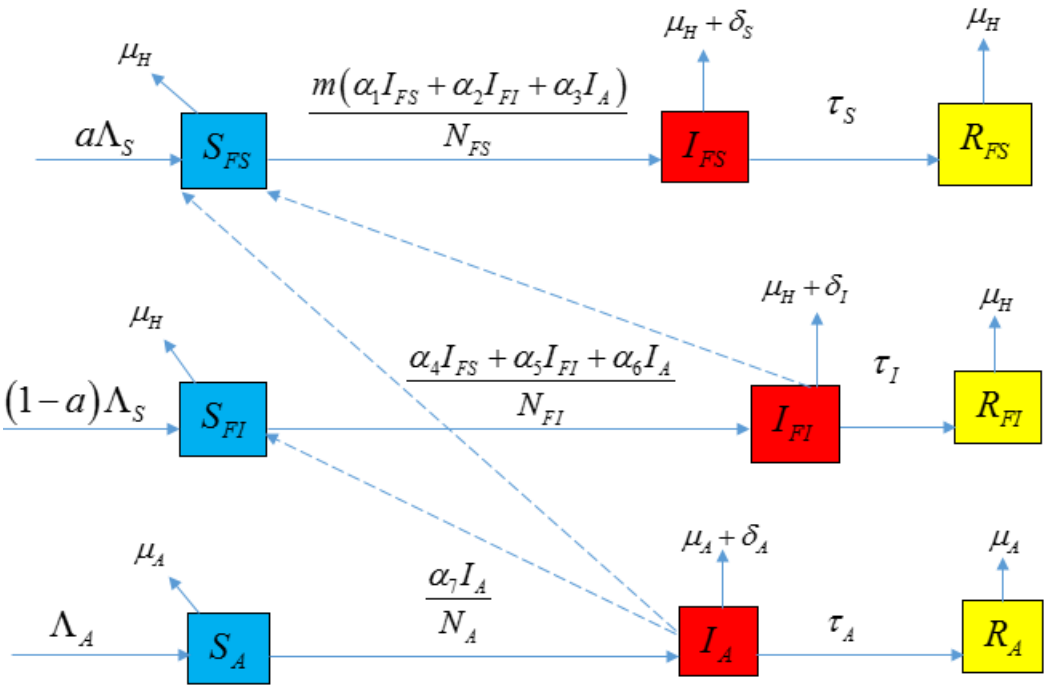

FIGURE 1. **Flow diagram for the Monkeypox model**

2.1. Invariant Region of the Monkeypox Model.

Theorem 2.1. *The solutions of the monkeypox model given in Eq. (6) are feasible for all $t > 0$ if they remain in the invariant region $\Omega = \Omega_1 \times \Omega_2 \subset \mathbb{R}^6_+ \times \mathbb{R}^3_+$, where Ω_1 and Ω_2 are positively invariant subsets for human and animal populations, respectively.*

To prove feasibility, we demonstrate that all solutions are uniformly bounded within Ω. Let:

$$\Omega_1 = \left\{ (S_{FS}, I_{FS}, R_{FS}, S_{FI}, I_{FI}, R_{FI}) \in \mathbb{R}^6_+ : S_{FS}, I_{FS}, R_{FS}, S_{FI}, I_{FI}, R_{FI} \geq 0 \right\},$$

$$\Omega_2 = \left\{ (S_A, I_A, R_A) \in \mathbb{R}^3_+ : S_A, I_A, R_A \geq 0 \right\}.$$

The total human population is:

$$N_H(t) = S_{FS}(t) + I_{FS}(t) + R_{FS}(t) + S_{FI}(t) + I_{FI}(t) + R_{FI}(t).$$

Where $N_H = N_{FS} + N_{FI}$.

Differentiating with respect to time, we get:

$$\frac{dN_H}{dt} = a\Lambda_S - \mu_H N_H(t) - \delta_S I_{FS}(t) - \delta_I I_{FI}(t).$$

Using the integrating factor method and initial condition $N_H(0) = N_H^0$, we solve:

$$N_H(t) \leq \frac{a\Lambda_S}{\mu_H} + \left(N_H^0 - \frac{a\Lambda_S}{\mu_H}\right) e^{-\mu_H t}.$$

As $t \to \infty$, $N_H(t)$ approaches $\frac{a\Lambda_S}{\mu_H}$. Therefore:

$$0 \leq N_H(t) \leq \frac{a\Lambda_S}{\mu_H}.$$

This shows that Ω_1 is positively invariant.

The total animal population is:

$$N_A(t) = S_A(t) + I_A(t) + R_A(t).$$

Differentiating with respect to time, we get:

$$\frac{dN_A}{dt} = \Lambda_A - \mu_A N_A(t) - \delta_A I_A(t).$$

Using the integrating factor method and initial condition $N_A(0) = N_A^0$, we solve:

$$N_A(t) \leq \frac{\Lambda_A}{\mu_A} + \left(N_A^0 - \frac{\Lambda_A}{\mu_A}\right) e^{-\mu_A t}.$$

As $t \to \infty$, $N_A(t)$ approaches $\frac{\Lambda_A}{\mu_A}$. Therefore:

$$0 \leq N_A(t) \leq \frac{\Lambda_A}{\mu_A}.$$

This shows that Ω_2 is positively invariant.

Since $N_H(t)$ and $N_A(t)$ are bounded and non-negative, all solutions of the system remain in the invariant region Ω. Thus, the model defined by Eq. (6) is feasible.

2.2. Positivity of Solutions for the Monkeypox Model.

Theorem 2.2. *Let the initial data for the monkeypox model given in* (6) *satisfy*

$$S_{FS}(0) > 0, I_{FS}(0) > 0, R_{FS}(0) > 0,$$

$$S_{FI}(0) > 0, I_{FI}(0) > 0, R_{FI}(0) > 0,$$

$$S_A(0) > 0, I_A(0) > 0, R_A(0) > 0.$$

Then, the solutions

$$S_{FS}(t), I_{FS}(t), R_{FS}(t), S_{FI}(t), I_{FI}(t), R_{FI}(t), S_A(t), I_A(t), R_A(t)$$

remain non-negative for all $t > 0$.

We will prove positivity for $S_{FS}(t)$, the susceptible population in the first subgroup. The same technique applies to all other compartments.

The differential equation for S_{FS} is

$$\frac{dS_{FS}}{dt} = a\Lambda_S - \frac{m(\alpha_1 I_{FS} + \alpha_2 I_{FI} + \alpha_3 I_A)}{N_{FS}} S_{FS} - \mu_H S_{FS}.$$

Rewriting,

$$\frac{dS_{FS}}{dt} \geq -\left(\frac{m(\alpha_1 I_{FS} + \alpha_2 I_{FI} + \alpha_3 I_A)}{N_{FS}} + \mu_H\right) S_{FS}.$$

Dividing through by S_{FS} (assuming $S_{FS} > 0$),

$$\int \frac{1}{S_{FS}} dS_{FS} \geq -\int \left(\frac{m(\alpha_1 I_{FS} + \alpha_2 I_{FI} + \alpha_3 I_A)}{N_{FS}} + \mu_H\right) dt.$$

Integrating,

$$\ln S_{FS} \geq -\int \left(\frac{m(\alpha_1 I_{FS} + \alpha_2 I_{FI} + \alpha_3 I_A)}{N_{FS}} + \mu_H\right) dt + C,$$

where C is the integration constant.

Exponentiating both sides,

$$S_{FS}(t) \geq C \exp\left(-\int \left(\frac{m(\alpha_1 I_{FS} + \alpha_2 I_{FI} + \alpha_3 I_A)}{N_{FS}} + \mu_H\right) dt\right).$$

At the initial condition, $t = 0$, we have $S_{FS}(0) = C > 0$. Thus,

$$S_{FS}(t) \geq S_{FS}(0) \exp\left(- \int \left(\frac{m\left(\alpha_1 I_{FS} + \alpha_2 I_{FI} + \alpha_3 I_A\right)}{N_{FS}} + \mu_H \right) dt \right) \geq 0.$$

Using similar steps for I_{FS}, R_{FS}, S_{FI}, I_{FI}, R_{FI}, S_A, I_A, and R_A, we obtain

$$S_{FS}(t), I_{FS}(t), R_{FS}(t), S_{FI}(t), I_{FI}(t), R_{FI}(t), S_A(t), I_A(t), R_A(t) \geq 0 \quad \text{for all } t > 0.$$

Thus, all compartments remain non-negative for all $t > 0$.

2.3. Asymptotic stability of the disease free equilibrium point of the Monkeypox model. The disease free equilibrium point of the Monkeypox model is the point where there is no disease in the population. This is the point where $I_{FS} = R_{FS} = I_{FI} = R_{FI} = I_A = R_A = 0$ as well as their associated parameters. Hence, the disease free equilibrium point of the Monkeypox model is given as:

$$\varepsilon_0 = (S^*_{FS}, I^*_{FS}, R^*_{FS}, S^*_{FI}, I^*_{FI}, R^*_{FI}, S^*_A, I^*_A, R^*_A) = \left(\frac{a\Lambda_S}{\mu_H}, 0, 0, \frac{(1-a)\Lambda_S}{\mu_H}, 0, 0, \frac{\Lambda_A}{\mu_A}, 0, 0 \right)$$

Thus, at the disease free equilibrium point of the Monkeypox model in (6), we have that

$$S^*_{FS} = N^*_{FS}, S^*_{FI} = N^*_{FI}, S^*_A = N^*_A.$$

2.4. Basic reproduction number of the Monkeypox model. The basic reproduction number (R_0) is the threshold parameter that measures the average number of secondary cases of infection caused by the introduction of a single infected individual into a wholly susceptible population. The basic reproduction number of the monkeypox model is determined using the next generation operator matrix method. It is defined as:

$$R_0 = \rho F V^{-1}$$

where F is defined as the matrix of new infections while$V$ is defined as the matrix of the transition term. ρ is the dominant eigenvalue of FV^{-1} matrix. For the monkeypox model in equation (6), we have

$$F = \begin{bmatrix} m\alpha_1 & m\alpha_2 & m\alpha_2 \\ \alpha_4 & \alpha_5 & \alpha_6 \\ 0 & 0 & \alpha_7 \end{bmatrix}, V = \begin{bmatrix} (\tau_S + \mu_H + \delta_S) & 0 & 0 \\ 0 & (\tau_I + \mu_H + \delta_I) & 0 \\ 0 & 0 & (\tau_A + \mu_A + \delta_A) \end{bmatrix}$$

$$FV^{-1} = \begin{bmatrix} \frac{m\alpha_1}{\tau_S+\mu_H+\delta_S} & \frac{m\alpha_2}{\tau_I+\mu_H+\delta_I} & \frac{m\alpha_3}{\tau_A+\mu_H+\delta_A} \\ \frac{\alpha_4}{\tau_S+\mu_H+\delta_S} & \frac{\alpha_5}{\tau_I+\mu_H+\delta_I} & \frac{\alpha_7}{\tau_A+\mu_H+\delta_A} \\ 0 & 0 & \frac{\alpha_7}{\tau_A+\mu_H+\delta_A} \end{bmatrix}$$

Thus, the basic reproduction numbers of the Monkeypox model are:

$$R_{0S} = \frac{(m\alpha_1+\alpha_5)\mu_H+m(\tau_I+\delta_I)\alpha_1+(\tau_S+\delta_S)\alpha_5+\sqrt{\alpha_1^2(\tau_I+\mu_H+\delta_I)^2m^2-2(\alpha_5\alpha_1-2\alpha_2\alpha_4)(\tau_I+\mu_H+\delta_I)(\tau_S+\mu_H+\delta_S)m+\alpha_5^2(\tau_S+\mu_H+\delta_S)^2}}{2(\tau_S+\mu_H+\delta_S)(\tau_I+\mu_H+\delta_I)}$$

$$R_{0I} = \frac{(m\alpha_1+\alpha_5)\mu_H+m(\tau_I+\delta_I)\alpha_1+(\tau_S+\delta_S)\alpha_5-\sqrt{\alpha_1^2(\tau_I+\mu_H+\delta_I)^2m^2-2(\alpha_5\alpha_1-2\alpha_2\alpha_4)(\tau_I+\mu_H+\delta_I)(\tau_S+\mu_H+\delta_S)m+\alpha_5^2(\tau_S+\mu_H+\delta_S)^2}}{2(\tau_S+\mu_H+\delta_S)(\tau_I+\mu_H+\delta_I)}$$

$$R_{0A} = \frac{\alpha_7}{\tau_A+\mu_H+\delta_A}$$

Where R_{0S}, R_{0I} and R_{0A} are the basic reproduction number of Monkeypox in the food-secure humans, food-insecure humans and animal population respectively.

2.5. Local Asymptotic stability of the disease free equilibrium point of the Monkeypox model.

Theorem 2.3. *The disease free equilibrium point of the Monkeypox model (6) is locally asymptotically stable whenever* $R_{0S} < 1, R_{0I} < 1,$ *and* $R_{0A} < 1$.

We use the Jacobian matrix of the Monkeypox model in (6) to prove the local asymptotic stability of its disease free equilibrium point. The Jacobian matrix of the Monkeypox model evaluated at its disease free equilibrium point is given as

$$J(\varepsilon_0) = \begin{bmatrix} -\mu_H & -m\alpha_1 & 0 & 0 & -m\alpha_2 & 0 & 0 & m\alpha_3 & 0 \\ 0 & m\alpha_1-(\tau_S+\mu_H+\delta_S) & 0 & 0 & m\alpha_2 & 0 & 0 & m\alpha_3 & 0 \\ 0 & \tau_S & -\mu_H & 0 & 0 & 0 & 0 & 0 & 0 \\ 0 & -\alpha_4 & 0 & -\mu_H & -\alpha_5 & 0 & 0 & -\alpha_6 & 0 \\ 0 & \alpha_4 & 0 & 0 & \alpha_5-(\tau_A+\mu_H+\delta_A) & 0 & 0 & \alpha_6 & 0 \\ 0 & 0 & 0 & 0 & -\mu_H & -\mu_H & 0 & 0 & 0 \\ 0 & 0 & 0 & 0 & 0 & 0 & -\mu_A & -\alpha_7 & 0 \\ 0 & 0 & 0 & 0 & 0 & 0 & 0 & \alpha_7-(\tau_A+\mu_A+\delta_A) & 0 \\ 0 & 0 & 0 & 0 & 0 & 0 & 0 & \tau_A & -\mu_A \end{bmatrix}$$

Using the row-column reduction method, which eliminates the first, third, fourth, sixth, seventh, and ninth columns and rows of $J(\varepsilon_0)$, it is implied that the first six eigenvalues of $J(\varepsilon_0)$ are μ_H (quadruple) and μ_A (twice).

The Jacobian matrix $J(\varepsilon_0)$ reduces to:

$$J_1(\varepsilon_0) = \begin{bmatrix} m\alpha_1 - (\tau_S + \mu_H + \delta_S) & m\alpha_2 & m\alpha_3 \\ \alpha_4 & \alpha_5 - (\tau_I + \mu_H + \delta_I) & \alpha_6 \\ 0 & 0 & \alpha_7 - (\tau_A + \mu_A + \delta_A) \end{bmatrix}$$

The characteristic polynomial of the Jacobian matrix $(J_1(\varepsilon_0))$ is obtained as

$$\begin{aligned} p(\lambda) &= \lambda^3 + b_2\lambda^2 + b_1\lambda + b_0 \\ &= \lambda^3 + \left[-\left(\frac{\tau_S + \mu_H + \delta_S}{\tau_S + \mu_H + \delta_S} + \frac{\tau_I + \mu_H + \delta_I}{\tau_I + \mu_H + \delta_I} + \frac{\tau_A + \mu_H + \delta_A}{\tau_A + \mu_H + \delta_A} \right) \right] \lambda^2 \\ &\quad + \left[(1 - R_{0S}) \frac{\tau_I + \mu_H + \delta_I}{\tau_S + \mu_H + \delta_S} + (1 - R_{0I}) \frac{\tau_S + \mu_H + \delta_S}{\tau_I + \mu_H + \delta_I} + (1 - R_{0A}) \frac{1}{\tau_A + \mu_H + \delta_A} \right] \lambda \\ &\quad + (1 - R_{0S})(1 - R_{0I}) + (1 - R_{0S})(1 - R_{0A}) + (1 - R_{0I})(1 - R_{0A}). \end{aligned} \tag{7}$$

Applying the Routh-Hurwitz criterion which ensures that for the Jacobian matrix of $(J_1(\varepsilon_0))$ to have negative real parts, its is necessary and sufficient that the co-efficients of λ in (7) exceed zero.

Thus, it implies that

$(1 - R_{0S}) > 0, (1 - R_{0I}) > 0, (1 - R_{0A}) > 0$ and $R_{0S} < 1, R_{0I} < 1$ and $R_{0A} < 1$.

Hence, the Monkeypox model in system (6) is locally asymptotically stable.

2.6. Fractional Monkeypox Mathematical Model. We extend in this section the integer model presented in equation (6) as given below:

$$\left.\begin{aligned} D_t S_{FS}(t) &= a\Lambda_S - \tfrac{m(\alpha_1 I_{FS} + \alpha_2 I_{FI} + \alpha_3 I_A)}{N_{FS}} S_{FS} - \mu_H S_{FS}, \\ D_t I_{FS}(t) &= \tfrac{m(\alpha_1 I_{FS} + \alpha_2 I_{FI} + \alpha_3 I_A)}{N_{FS}} S_{FS} - (\tau_S + \delta_S + \mu_H) I_{FS}, \\ D_t R_{FS}(t) &= \tau_S I_{FS} - \mu_H R_{FS}, \\ D_t S_{FI}(t) &= (1 - a)\Lambda_S - \tfrac{(\alpha_4 I_{FS} + \alpha_5 I_{FI} + \alpha_6 I_A)}{N_{FI}} S_{FI} - \mu_H S_{FI}, \\ D_t I_{FI}(t) &= \tfrac{\alpha_4 I_{FS} + \alpha_5 I_{FI} + \alpha_6 I_A}{N_{FI}} S_{FI} - (\tau_I + \delta_I + \mu_H) I_{FI}, \\ D_t R_{FI}(t) &= \tau_I I_{FI} - \mu_H R_{FI}, \\ D_t S_A(t) &= \Lambda_A - \tfrac{\alpha_7 I_A}{N_A} S_A - \mu_A S_A, \\ D_t I_A(t) &= \tfrac{\alpha_7 I_A}{N_A} S_A - (\tau_A + \delta_A + \mu_A) I_A, \\ D_t R_A(t) &= \tau_A I_A - \mu_A R_A. \end{aligned}\right\} \tag{8}$$

With initial conditions

$$S_{FS0}(t) = S_{FS}(0), I_{FS0}(t) = I_{FS}(0), R_{FS0}(t) = R_{FS}(0),$$
$$S_{FI0}(t) = S_{FI}(0), I_{FI0}(t) = I_{FI}(0), R_{FI0}(t) = R_{FI}(0),$$
$$S_{A0}(t) = S_A(0), I_{A0}(t) = I_A(0), R_{A0}(t) = R_A(0).$$

Model (8) is therefore re-modeled by replacing the classical derivative D_t with ${}_0^C D_t^\theta$, ${}_0^{CF} D_t^\theta$, and ${}_0^{ABC} D_t^\theta$, which represent the Caputo derivative of fractional order θ, the Caputo-Fabrizio derivative of fractional order θ, and the Atagana-Baleanu derivative of fractional order θ, respectively. The modified Monkeypox model using the Caputo derivative of fractional order θ with a power law is given as:

$$\left.\begin{aligned}
{}_0^C D_t^\theta S_{FS}(t) &= a\Lambda_S - \tfrac{m(\alpha_1 I_{FS}+\alpha_2 I_{FI}+\alpha_3 I_A)}{N_{FS}} S_{FS} - \mu_H S_{FS},\\
{}_0^C D_t^\theta I_{FS}(t) &= \tfrac{m(\alpha_1 I_{FS}+\alpha_2 I_{FI}+\alpha_3 I_A)}{N_{FS}} S_{FS} - (\tau_S + \delta_S + \mu_H) I_{FS},\\
{}_0^C D_t^\theta R_{FS}(t) &= \tau_S I_{FS} - \mu_H R_{FS},\\
{}_0^C D_t^\theta S_{FI}(t) &= (1-a)\Lambda_S - \tfrac{(\alpha_4 I_{FS}+\alpha_5 I_{FI}+\alpha_6 I_A)}{N_{FI}} S_{FI} - \mu_H S_{FI},\\
{}_0^C D_t^\theta I_{FI}(t) &= \tfrac{\alpha_4 I_{FS}+\alpha_5 I_{FI}+\alpha_6 I_A}{N_{FI}} S_{FI} - (\tau_I + \delta_I + \mu_H) I_{FI},\\
{}_0^C D_t^\theta R_{FI}(t) &= \tau_I I_{FI} - \mu_H R_{FI},\\
{}_0^C D_t^\theta S_A(t) &= \Lambda_A - \tfrac{\alpha_7 I_A}{N_A} S_A - \mu_A S_A,\\
{}_0^C D_t^\theta I_A(t) &= \tfrac{\alpha_7 I_A}{N_A} S_A - (\tau_A + \delta_A + \mu_A) I_A,\\
{}_0^C D_t^\theta R_A(t) &= \tau_A I_A - \mu_A R_A.
\end{aligned}\right\} \tag{9}$$

The modified Monkeypox model with Caputo-Fabrizio derivative with fractional order θ having an exponential kernel law is presented as:

$$
\left.\begin{aligned}
&{}_0^{CF}D_t^{\theta}S_{FS}(t) = a\Lambda_S - \tfrac{m(\alpha_1 I_{FS}+\alpha_2 I_{FI}+\alpha_3 I_A)}{N_{FS}}S_{FS} - \mu_H S_{FS},\\
&{}_0^{CF}D_t^{\theta}I_{FS}(t) = \tfrac{m(\alpha_1 I_{FS}+\alpha_2 I_{FI}+\alpha_3 I_A)}{N_{FS}}S_{FS} - (\tau_S+\delta_S+\mu_H)I_{FS},\\
&{}_0^{CF}D_t^{\theta}R_{FS}(t) = \tau_S I_{FS} - \mu_H R_{FS},\\
&{}_0^{CF}D_t^{\theta}S_{FI}(t) = (1-a)\Lambda_S - \tfrac{(\alpha_4 I_{FS}+\alpha_5 I_{FI}+\alpha_6 I_A)}{N_{FI}}S_{FI} - \mu_H S_{FI},\\
&{}_0^{CF}D_t^{\theta}I_{FI}(t) = \tfrac{\alpha_4 I_{FS}+\alpha_5 I_{FI}+\alpha_6 I_A}{N_{FI}}S_{FI} - (\tau_I+\delta_I+\mu_H)I_{FI},\\
&{}_0^{CF}D_t^{\theta}R_{FI}(t) = \tau_I I_{FI} - \mu_H R_{FI},\\
&{}_0^{CF}D_t^{\theta}S_A(t) = \Lambda_A - \tfrac{\alpha_7 I_A}{N_A}S_A - \mu_A S_A,\\
&{}_0^{CF}D_t^{\theta}I_A(t) = \tfrac{\alpha_7 I_A}{N_A}S_A - (\tau_A+\delta_A+\mu_A)I_A,\\
&{}_0^{CF}D_t^{\theta}R_A(t) = \tau_A I_A - \mu_A R_A.
\end{aligned}\right\} \tag{10}
$$

Also the modified Monkeypox model with Atagana-Baleanu-derivative with generalized Mittag-Leffler function is presented as:

$$
\left.\begin{aligned}
&{}_0^{ABC}D_t^{\theta}S_{FS}(t) = a\Lambda_S - \tfrac{m(\alpha_1 I_{FS}+\alpha_2 I_{FI}+\alpha_3 I_A)}{N_{FS}}S_{FS} - \mu_H S_{FS},\\
&{}_0^{ABC}D_t^{\theta}I_{FS}(t) = \tfrac{m(\alpha_1 I_{FS}+\alpha_2 I_{FI}+\alpha_3 I_A)}{N_{FS}}S_{FS} - (\tau_S+\delta_S+\mu_H)I_{FS},\\
&{}_0^{ABC}D_t^{\theta}R_{FS}(t) = \tau_S I_{FS} - \mu_H R_{FS},\\
&{}_0^{ABC}D_t^{\theta}S_{FI}(t) = (1-a)\Lambda_S - \tfrac{(\alpha_4 I_{FS}+\alpha_5 I_{FI}+\alpha_6 I_A)}{N_{FI}}S_{FI} - \mu_H S_{FI},\\
&{}_0^{ABC}D_t^{\theta}I_{FI}(t) = \tfrac{\alpha_4 I_{FS}+\alpha_5 I_{FI}+\alpha_6 I_A}{N_{FI}}S_{FI} - (\tau_I+\delta_I+\mu_H)I_{FI},\\
&{}_0^{ABC}D_t^{\theta}R_{FI}(t) = \tau_I I_{FI} - \mu_H R_{FI},\\
&{}_0^{ABC}D_t^{\theta}S_A(t) = \Lambda_A - \tfrac{\alpha_7 I_A}{N_A}S_A - \mu_A S_A,\\
&{}_0^{ABC}D_t^{\theta}I_A(t) = \tfrac{\alpha_7 I_A}{N_A}S_A - (\tau_A+\delta_A+\mu_A)I_A,\\
&{}_0^{ABC}D_t^{\theta}R_A(t) = \tau_A I_A - \mu_A R_A.
\end{aligned}\right\} \tag{11}
$$

3. Numerical Method for the Caputo Derivative

We provided a concise overview of a Predictor-Corrector numerical method designed to address the Monkeypox model incorporating the Caputo fractional derivative of order θ.

$$
\left.\begin{aligned}
&{}_0^{C}D_t^{\theta}x(t) = F(t,x(t)), 0 \le t \le T,\\
&x^{(n)}(0) = x_0^{(n)}, n = 0,1,2,...k-1.
\end{aligned}\right\} \tag{12}
$$

Equation (12) is equivalent to the Volterra integral equation.

$$x(t)=\sum_{n=0}^{|\theta|-1}x_0^{(n)}\frac{t^n}{n!}+\frac{1}{\left|\overline{(\theta)}\right|}\int_0^t\frac{F(\psi,x(\psi))}{(t-\psi)^{1-\theta}}d\psi, \tag{13}$$

Setting $P=\frac{T}{N}$, $t_r=rp,(r=0,1,2,3,...R)$.

We therefore discretized equation (13) as follows:

$$x_p(t_{r+1})=\sum_{n=0}^{|\theta|-1}\frac{t_{r+1}^n}{n!}x_0^{(n)}+\frac{P^\theta}{\left|\overline{(\theta+2)}\right|}\left[F\left(t_{r+1},x_P^V(t_{r+1})\right)+\sum_{i=0}^{k}b_{i,k+1}F(t_i,x_r(t_i))\right] \tag{14}$$

Here, $x_p(t_{r+1})$ refers to the predicted value, calculated using the generalized Adams-Bashforth method as outlined below:

$$x_P^V(t_{r+1})=\sum_{n=0}^{|\theta|-1}\frac{t_{r+1}^n}{n!}x_0^{(n)}+\frac{1}{\left|\overline{(\theta)}\right|}\sum_{i=0}^{k}d_{i,k+1}F(t_i,x_r(t_i)) \tag{15}$$

Where

$$b_{i,k+1}=\begin{cases}r^{\theta+1}-(r-\theta)(r+1)^\theta, i=0,\\ (r-i+2)^{\theta+1}+(r-i)^{\theta+1}-2(r-i+1)^{\theta+1}, 1\le i\le r,\\ 1.i=r+1.\end{cases}$$

and

$$d_{i,k+1}=\frac{P^\theta}{\theta}\left((r+1-i)^\theta-(r-i)^\theta\right), 0\le i\le k, i=1,2,3.$$

3.1. Predictor-Corrector Numerical Method for the Monkeypox model with Caputo Fractional derivative. To solve the fractional operator in our model (9), we apply the predictor-corrector numerical approach. For this purpose, model (9) is discretized as shown below:

$$\begin{aligned}S_{FSr+1}=S_{FS}(0)+\frac{P^\theta}{\left|\overline{(\theta+2)}\right|}\Big[&F_1(t_{r+1},S_{FSr+1}^V,I_{FSr+1}^V,R_{FSr+1}^V,S_{FIr+1}^V,I_{FIr+1}^V,R_{FIr+1}^V,S_{Ar+1}^V,I_{Ar+1}^V,R_{Ar+1}^V)\\ &+\sum_{i=0}^{k}b_{i,k+1}F_1(t_i,S_{FSi},I_{FSi},R_{FSi},S_{FIi},I_{FIi},R_{FIi},S_{Ai},I_{Ai},R_{Ai})\Big],\\ I_{FSr+1}=I_{FS}(0)+\frac{P^\theta}{\left|\overline{(\theta+2)}\right|}\Big[&F_2(t_{r+1},S_{FSr+1}^V,I_{FSr+1}^V,R_{FSr+1}^V,S_{FIr+1}^V,I_{FIr+1}^V,R_{FIr+1}^V,S_{Ar+1}^V,I_{Ar+1}^V,R_{Ar+1}^V)\\ &+\sum_{i=0}^{k}b_{i,k+1}F_2(t_i,S_{FSi},I_{FSi},R_{FSi},S_{FIi},I_{FIi},R_{FIi},S_{Ai},I_{Ai},R_{Ai})\Big],\end{aligned}$$

$$
\begin{aligned}
R_{FSr+1} &= R_{FS}(0) + \frac{P^{\theta}}{\left|\overline{(\theta+2)}\right|}\Big[F_3(t_{r+1}, S^V_{FSr+1}, I^V_{FSr+1}, R^V_{FSr+1}, S^V_{FIr+1}, I^V_{FIr+1}, R^V_{FIr+1}, S^V_{Ar+1}, I^V_{Ar+1}, R^V_{Ar+1}) \\
&\quad + \sum_{i=0}^{k} b_{i,k+1} F_3(t_i, S_{FSi}, I_{FSi}, R_{FSi}, S_{FIi}, I_{FIi}, R_{FIi}, S_{Ai}, I_{Ai}, R_{Ai})\Big]. \\
S_{FIr+1} &= S_{FI}(0) + \frac{P^{\theta}}{\left|\overline{(\theta+2)}\right|}\Big[F_4(t_{r+1}, S^V_{FSr+1}, I^V_{FSr+1}, R^V_{FSr+1}, S^V_{FIr+1}, I^V_{FIr+1}, R^V_{FIr+1}, S^V_{Ar+1}, I^V_{Ar+1}, R^V_{Ar+1}) \\
&\quad + \sum_{i=0}^{k} b_{i,k+1} F_4(t_i, S_{FSi}, I_{FSi}, R_{FSi}, S_{FIi}, I_{FIi}, R_{FIi}, S_{Ai}, I_{Ai}, R_{Ai})\Big], \\
I_{FIr+1} &= I_{FI}(0) + \frac{P^{\theta}}{\left|\overline{(\theta+2)}\right|}\Big[F_5(t_{r+1}, S^V_{FSr+1}, I^V_{FSr+1}, R^V_{FSr+1}, S^V_{FIr+1}, I^V_{FIr+1}, R^V_{FIr+1}, S^V_{Ar+1}, I^V_{Ar+1}, R^V_{Ar+1}) \\
&\quad + \sum_{i=0}^{k} b_{i,k+1} F_5(t_i, S_{FSi}, I_{FSi}, R_{FSi}, S_{FIi}, I_{FIi}, R_{FIi}, S_{Ai}, I_{Ai}, R_{Ai})\Big], \\
R_{FIr+1} &= R_{FI}(0) + \frac{P^{\theta}}{\left|\overline{(\theta+2)}\right|}\Big[F_6(t_{r+1}, S^V_{FSr+1}, I^V_{FSr+1}, R^V_{FSr+1}, S^V_{FIr+1}, I^V_{FIr+1}, R^V_{FIr+1}, S^V_{Ar+1}, I^V_{Ar+1}, R^V_{Ar+1}) \\
&\quad + \sum_{i=0}^{k} b_{i,k+1} F_6(t_i, S_{FSi}, I_{FSi}, R_{FSi}, S_{FIi}, I_{FIi}, R_{FIi}, S_{Ai}, I_{Ai}, R_{Ai})\Big], \\
S_{Ar+1} &= S_A(0) + \frac{P^{\theta}}{\left|\overline{(\theta+2)}\right|}\Big[F_7(t_{r+1}, S^V_{FSr+1}, I^V_{FSr+1}, R^V_{FSr+1}, S^V_{FIr+1}, I^V_{FIr+1}, R^V_{FIr+1}, S^V_{Ar+1}, I^V_{Ar+1}, R^V_{Ar+1}) \\
&\quad + \sum_{i=0}^{k} b_{i,k+1} F_7(t_i, S_{FSi}, I_{FSi}, R_{FSi}, S_{FIi}, I_{FIi}, R_{FIi}, S_{Ai}, I_{Ai}, R_{Ai})\Big], \\
I_{Ar+1} &= I_A(0) + \frac{P^{\theta}}{\left|\overline{(\theta+2)}\right|}\Big[F_8(t_{r+1}, S^V_{FSr+1}, I^V_{FSr+1}, R^V_{FSr+1}, S^V_{FIr+1}, I^V_{FIr+1}, R^V_{FIr+1}, S^V_{Ar+1}, I^V_{Ar+1}, R^V_{Ar+1}) \\
&\quad + \sum_{i=0}^{k} b_{i,k+1} F_8(t_i, S_{FSi}, I_{FSi}, R_{FSi}, S_{FIi}, I_{FIi}, R_{FIi}, S_{Ai}, I_{Ai}, R_{Ai})\Big], \\
R_{Ar+1} &= R_A(0) + \frac{P^{\theta}}{\left|\overline{(\theta+2)}\right|}\Big[F_9(t_{r+1}, S^V_{FSr+1}, I^V_{FSr+1}, R^V_{FSr+1}, S^V_{FIr+1}, I^V_{FIr+1}, R^V_{FIr+1}, S^V_{Ar+1}, I^V_{Ar+1}, R^V_{Ar+1}) \\
&\quad + \sum_{i=0}^{k} b_{i,k+1} F_9(t_i, S_{FSi}, I_{FSi}, R_{FSi}, S_{FIi}, I_{FIi}, R_{FIi}, S_{Ai}, I_{Ai}, R_{Ai})\Big].
\end{aligned}
\tag{16}
$$

$S^V_{FSr+1}, I^V_{FSr+1}, R^V_{FSr+1}, S^V_{FIr+1}, I^V_{FIr+1}, R^V_{FIr+1}, S^V_{Ar+1}, I^V_{Ar+1}, R^V_{Ar+1}$, are therefore written as follows:

$$
\left.
\begin{aligned}
S^V_{FSr+1} &= S_{FS}(0) + \tfrac{1}{|(\theta)|}\left[\sum_{i=0}^{k} d_{i,k+1} F_1\left(t_i, S_{FSi}, I_{FSi}, R_{FSi}, S_{FIi}, I_{FIi}, R_{FIi}, S_{Ai}, I_{Ai}, R_{Ai}\right)\right],\\
I^V_{FSr+1} &= I_{FS}(0) + \tfrac{1}{|(\theta)|}\left[\sum_{i=0}^{k} d_{i,k+1} F_2\left(t_i, S_{FSi}, I_{FSi}, R_{FSi}, S_{FIi}, I_{FIi}, R_{FIi}, S_{Ai}, I_{Ai}, R_{Ai}\right)\right],\\
R^V_{FSr+1} &= R_{FS}(0) + \tfrac{1}{|(\theta)|}\left[\sum_{i=0}^{k} d_{i,k+1} F_3\left(t_i, S_{FSi}, I_{FSi}, R_{FSi}, S_{FIi}, I_{FIi}, R_{FIi}, S_{Ai}, I_{Ai}, R_{Ai}\right)\right],\\
S^V_{FIr+1} &= S_{FI}(0) + \tfrac{1}{|(\theta)|}\left[\sum_{i=0}^{k} d_{i,k+1} F_4\left(t_i, S_{FSi}, I_{FSi}, R_{FSi}, S_{FIi}, I_{FIi}, R_{FIi}, S_{Ai}, I_{Ai}, R_{Ai}\right)\right],\\
I^V_{FIr+1} &= I_{FI}(0) + \tfrac{1}{|(\theta)|}\left[\sum_{i=0}^{k} d_{i,k+1} F_5\left(t_i, S_{FSi}, I_{FSi}, R_{FSi}, S_{FIi}, I_{FIi}, R_{FIi}, S_{Ai}, I_{Ai}, R_{Ai}\right)\right],\\
R^V_{FIr+1} &= R_{FI}(0) + \tfrac{1}{|(\theta)|}\left[\sum_{i=0}^{k} d_{i,k+1} F_6\left(t_i, S_{FSi}, I_{FSi}, R_{FSi}, S_{FIi}, I_{FIi}, R_{FIi}, S_{Ai}, I_{Ai}, R_{Ai}\right)\right],\\
S^V_{Ar+1} &= S_A(0) + \tfrac{1}{|(\theta)|}\left[\sum_{i=0}^{k} d_{i,k+1} F_7\left(t_i, S_{FSi}, I_{FSi}, R_{FSi}, S_{FIi}, I_{FIi}, R_{FIi}, S_{Ai}, I_{Ai}, R_{Ai}\right)\right],\\
I^V_{Ar+1} &= I_A(0) + \tfrac{1}{|(\theta)|}\left[\sum_{i=0}^{k} d_{i,k+1} F_8\left(t_i, S_{FSi}, I_{FSi}, R_{FSi}, S_{FIi}, I_{FIi}, R_{FIi}, S_{Ai}, I_{Ai}, R_{Ai}\right)\right],\\
R^V_{Ar+1} &= R_A(0) + \tfrac{1}{|(\theta)|}\left[\sum_{i=0}^{k} d_{i,k+1} F_9\left(t_i, S_{FSi}, I_{FSi}, R_{FSi}, S_{FIi}, I_{FIi}, R_{FIi}, S_{Ai}, I_{Ai}, R_{Ai}\right)\right].
\end{aligned}
\right\} \tag{17}
$$

Where,

(18)

$$
\left.
\begin{aligned}
F_1(t, S_{FS}, I_{FS}, R_{FS}, S_{FI}, I_{FI}, R_{FI}, S_A, I_A, R_A) &= a\Lambda_S - \tfrac{m(\alpha_1 I_{FS} + \alpha_2 I_{FI} + \alpha_3 I_A)}{N_{FS}} S_{FS} - \mu_H S_{FS},\\
F_2(t, S_{FS}, I_{FS}, R_{FS}, S_{FI}, I_{FI}, R_{FI}, S_A, I_A, R_A) &= \tfrac{m(\alpha_1 I_{FS} + \alpha_2 I_{FI} + \alpha_3 I_A)}{N_{FS}} S_{FS} - (\tau_S + \delta_S + \mu_H) I_{FS},\\
F_3(t, S_{FS}, I_{FS}, R_{FS}, S_{FI}, I_{FI}, R_{FI}, S_A, I_A, R_A) &= \tau_S I_{FS} - \mu_H R_{FS},\\
F_4(t, S_{FS}, I_{FS}, R_{FS}, S_{FI}, I_{FI}, R_{FI}, S_A, I_A, R_A) &= (1-a)\Lambda_S - \tfrac{(\alpha_4 I_{FS} + \alpha_5 I_{FI} + \alpha_6 I_A)}{N_{FI}} S_{FI} - \mu_H S_{FI},\\
F_5(t, S_{FS}, I_{FS}, R_{FS}, S_{FI}, I_{FI}, R_{FI}, S_A, I_A, R_A) &= \tfrac{(\alpha_4 I_{FS} + \alpha_5 I_{FI} + \alpha_6 I_A)}{N_{FI}} S_{FI} - (\tau_I + \delta_I + \mu_H) I_{FI},\\
F_6(t, S_{FS}, I_{FS}, R_{FS}, S_{FI}, I_{FI}, R_{FI}, S_A, I_A, R_A) &= \tau_I I_{FI} - \mu_H R_{FI},\\
F_7(t, S_{FS}, I_{FS}, R_{FS}, S_{FI}, I_{FI}, R_{FI}, S_A, I_A, R_A) &= \Lambda_A - \tfrac{\alpha_7 I_A}{N_A} S_A - \mu_A S_A,\\
F_8(t, S_{FS}, I_{FS}, R_{FS}, S_{FI}, I_{FI}, R_{FI}, S_A, I_A, R_A) &= \tfrac{\alpha_7 I_A}{N_A} S_A - (\tau_A + \delta_A + \mu_A) I_A,\\
F_9(t, S_{FS}, I_{FS}, R_{FS}, S_{FI}, I_{FI}, R_{FI}, S_A, I_A, R_A) &= \tau_A I_A - \mu_A R_A.
\end{aligned}
\right\}
$$

3.2. Existence and Uniqueness of Solutions for the Modified Monkeypox Model with Caputo-Fabrizio Derivative.

In this section, we employ the fixed point theorem to investigate the existence and uniqueness of solution for the modified Monkeypox model with Caputo-Fabrizio derivative presented in equation (10).

The model is therefore transformed into an integral equation given as:

$$
\begin{aligned}
S_{FS}(t)-S_{FS}(0) &=_0^{CF} I_t^{\theta}\left[a\Lambda_S-\frac{m(\alpha_1 I_{FS}+\alpha_2 I_{FI}+\alpha_3 I_A)}{N_{FS}}S_{FS}-\mu_H S_{FS}\right],\\
I_{FS}(t)-I_{FS}(0) &=_0^{CF} I_t^{\theta}\left[\frac{m(\alpha_1 I_{FS}+\alpha_2 I_{FI}+\alpha_3 I_A)}{N_{FS}}S_{FS}-(\tau_S+\delta_S+\mu_H)I_{FS}\right],\\
R_{FS}(t)-R_{FS}(0) &=_0^{CF} I_t^{\theta}\left[\tau_S I_{FS}-\mu_H R_{FS}\right],\\
S_{FI}(t)-S_{FI}(0) &=_0^{CF} I_t^{\theta}\left[(1-a)\Lambda_S-\frac{\alpha_4 I_{FS}+\alpha_5 I_{FI}+\alpha_6 I_A}{N_{FI}}S_{FI}-\mu_H S_{FI}\right],\\
I_{FI}(t)-I_{FI}(0) &=_0^{CF} I_t^{\theta}\left[\frac{\alpha_4 I_{FS}+\alpha_5 I_{FI}+\alpha_6 I_A}{N_{FI}}S_{FI}-(\tau_I+\delta_I+\mu_H)I_{FI}\right],\\
R_{FI}(t)-R_{FI}(0) &=_0^{CF} I_t^{\theta}\left[\tau_I I_{FI}-\mu_H R_{FI}\right],\\
S_A(t)-S_A(0) &=_0^{CF} I_t^{\theta}\left[\Lambda_A-\frac{\alpha_7 I_A}{N_A}S_A-\mu_A S_A\right],\\
I_A(t)-I_A(0) &=_0^{CF} I_t^{\theta}\left[\frac{\alpha_7 I_A}{N_A}S_A-(\tau_A+\delta_A+\mu_A)I_A\right],\\
R_A(t)-R_A(0) &=_0^{CF} I_t^{\theta}\left[\tau_A I_A-\mu_A R_A\right].
\end{aligned}
\tag{19}
$$

The kernel is defined as follows:

$$
\left.
\begin{aligned}
Y_1(t,S_{FS}) &= a\Lambda_S-\tfrac{m(\alpha_1 I_{FS}+\alpha_2 I_{FI}+\alpha_3 I_A)}{N_{FS}}S_{FS}-\mu_H S_{FS},\\
Y_2(t,E_{FS}) &= \tfrac{m(\alpha_1 I_{FS}+\alpha_2 I_{FI}+\alpha_3 I_A)}{N_{FS}}S_{FS}-(\alpha_1+\tau)E_{FS}-\mu_H E_{FS},\\
Y_3(t,R_{FS}) &= \tau_S I_{FS}-\mu_H R_{FS},\\
Y_4(t,S_{FI}) &= (1-a)\Lambda_S-\tfrac{(\alpha_4 I_{FS}+\alpha_5 I_{FI}+\alpha_6 I_A)}{N_{FI}}S_{FI}-\mu_H S_{FI},\\
Y_5(t,I_{FS}) &= \tfrac{\alpha_4 I_{FS}+\alpha_5 I_{FI}+\alpha_6 I_A}{N_{FI}}S_{FI}-(\tau_I+\delta_I+\mu_H)I_{FS}.
\end{aligned}
\right\}
$$

$$
\left.
\begin{aligned}
Y_6(t,R_{FI}) &= \tau_I I_{FI}-\mu_H R_{FI},\\
Y_7(t,S_A) &= \Lambda_A-\tfrac{\alpha_7 I_A}{N_A}S_A-\mu_A S_A,\\
Y_8(t,E_A) &= \tfrac{\alpha_7 I_A}{N_A}S_A-(\tau_A+\delta_A+\mu_A)I_A,\\
Y_9(t,Q_A) &= \tau_A I_A-\mu_A R_A.
\end{aligned}
\right\}
\tag{20}
$$

We obtained the following after using the arbitrary integral in equation (19).

$$
\left.\begin{aligned}
S_{FS}(t)-S_{FS}(0) &= \tfrac{2(i-\theta)}{(2-\theta)N(\theta)}Y_1(t,S_{FS})+\tfrac{2\theta}{(2-\theta)N(\theta)}\int_0^t Y_1(\phi,S_{FS})d\phi,\\
I_{FS}(t)-I_{FS}(0) &= \tfrac{2(i-\theta)}{(2-\theta)N(\theta)}Y_2(t,S_{FS})+\tfrac{2\theta}{(2-\theta)N(\theta)}\int_0^t Y_2(\phi,S_{FS})d\phi,\\
R_{FS}(t)-R_{FS}(0) &= \tfrac{2(i-\theta)}{(2-\theta)N(\theta)}Y_3(t,S_{FS})+\tfrac{2\theta}{(2-\theta)N(\theta)}\int_0^t Y_3(\phi,S_{FS})d\phi,\\
S_{FI}(t)-S_{FI}(0) &= \tfrac{2(i-\theta)}{(2-\theta)N(\theta)}Y_4(t,S_{FI})+\tfrac{2\theta}{(2-\theta)N(\theta)}\int_0^t Y_4(\phi,S_{FI})d\phi,\\
E_{FI}(t)-E_{FI}(0) &= \tfrac{2(i-\theta)}{(2-\theta)N(\theta)}Y_5(t,S_{FI})+\tfrac{2\theta}{(2-\theta)N(\theta)}\int_0^t Y_5(\phi,S_{FI})d\phi,\\
I_{FI}(t)-I_{FI}(0) &= \tfrac{2(i-\theta)}{(2-\theta)N(\theta)}Y_6(t,S_{FI})+\tfrac{2\theta}{(2-\theta)N(\theta)}\int_0^t Y_6(\phi,S_{FI})d\phi,\\
S_A(t)-S_A(0) &= \tfrac{2(i-\theta)}{(2-\theta)N(\theta)}Y_7(t,S_A)+\tfrac{2\theta}{(2-\theta)N(\theta)}\int_0^t Y_7(\phi,S_A)d\phi,\\
I_A(t)-I_A(0) &= \tfrac{2(i-\theta)}{(2-\theta)N(\theta)}Y_8(t,S_A)+\tfrac{2\theta}{(2-\theta)N(\theta)}\int_0^t Y_8(\phi,S_A)d\phi,\\
R_{FI}(t)-R_{FI}(0) &= \tfrac{2(i-\theta)}{(2-\theta)N(\theta)}Y_9(t,S_A)+\tfrac{2\theta}{(2-\theta)N(\theta)}\int_0^t Y_9(\phi,S_A)d\phi,
\end{aligned}\right\} \tag{21}
$$

Theorem 3.1. *The kernels Y_1, Y_2, Y_3, Y_4, Y_5, Y_6, Y_7, Y_8 and Y_9 in equation (20) fulfills the Lipschitz and contraction condition provided the inequality given below is satisfied.*

$$0 \leq m(\alpha_1 g_2 + \alpha_2 g_4 + \alpha_3 g_6 + \mu g_1) < 1$$

Starting with kernel Y_1. Assuming that kernel Y_1, has S and S^* as functions, then we can say

$$
\begin{aligned}
\left\|Y_1(t,S_{FS}) - Y_1\left(t,S^*_{FS}\right)\right\| &= \left\| -\tfrac{m(\alpha_1 I_{FS}+\alpha_2 I_{FI}+\alpha_3 I_A)}{N_{FS}} S_{FS} - S^*_{FS} \right\|,\\
&\leq m(\alpha_1 \|I_{FS}\| + \alpha_2 \|I_{FI}\| + \alpha_3 \|I_A\| + \mu)\left\|S_{FS} - S^*_{FS}\right\|,\\
&\leq m(\alpha_1 g_2 + \alpha_2 g_4 + \alpha_3 g_6 + \mu g_1)\left\|S_{FS} - S^*_{FS}\right\|.
\end{aligned} \tag{22}
$$

Let $L_1 = m(\alpha_1 g_2 + \alpha_2 g_4 + +\alpha_3 g_6 + \mu g_1)$.

Considering the fact that

$$\|S_{FS}\| \leq g_1, \|I_{FS}\| \leq g_2, \|R_{FS}\| \leq g_3, \|S_{FI}\| \leq g_4, \|I_{FI}\| \leq g_5,$$

$$\|R_{FI}\| \leq g_6, \|S_A\| \leq g_7, \|E_A\| \leq g_8, \|R_A\| \leq g_9$$

are functions that are bounded where $g_1, g_2, g_3, g_4, g_5, g_6, g_7, g_8$ and g_9 are some non-negative constants.

We therefore have that

$$\|Y_1(t,S_{FS}) - Y_1(t,S^*_{FS})\| \leq \rho_1 \|S_{FS} - S^*_{FS}\| \tag{23}$$

Equation (23) means kernel Y_1 satisfied the Lipschitz condition. For the contraction condition, $0 \leq \rho_1 < 1$ settles the case.

Similarly, we can write expressions for then remaining kernels as follows

$$
\begin{cases}
\left\|Y_2(t,I_{FS}) - Y_2\left(t,I^*_{FS}\right)\right\| \leq \rho_2 \left\|I_{FS} - I^*_{FS}\right\|, \\
\left\|Y_3(t,R_{FS}) - Y_3\left(t,R^*_{FS}\right)\right\| \leq \rho_3 \left\|R_{FS} - R^*_{FS}\right\|, \\
\left\|Y_4(t,S_{FI}) - Y_4(t,S^*_{FI})\right\| \leq \rho_4 \left\|S_{FI} - S^*_{FI}\right\|, \\
\left\|Y_5(t,I_{FI}) - Y_5(t,I^*_{FI})\right\| \leq \rho_5 \left\|I_{FI} - I^*_{FI}\right\|, \\
\left\|Y_6(t,R_{FI}) - Y_6(t,R^*_{FI})\right\| \leq \rho_6 \left\|R_{FI} - R^*_{FI}\right\|, \\
\left\|Y_7(t,S_A) - Y_7(t,S^*_A)\right\| \leq \rho_7 \left\|S_A - S^*_A\right\|, \\
\left\|Y_8(t,I_A) - Y_8(t,I^*_A)\right\| \leq \rho_8 \left\|I_A - I^*_A\right\|, \\
\left\|Y_9(t,R_A) - Y_9(t,R^*_A)\right\| \leq \rho_9 \left\|R_A - R^*_A\right\|
\end{cases} \tag{24}
$$

Introducing the recursive formula using equation (21) gives:

$$
\left.
\begin{aligned}
S_{FSr}(t) &= \tfrac{2(1-\theta)}{(2-\theta)N(\theta)} Y_1(t,S_{FSr-1}) + \tfrac{2\theta}{(2-\theta)N(\theta)} \int_0^t Y_1(\phi,S_{r-1})\, d\phi \\
I_{FSr}(t) &= \tfrac{2(1-\theta)}{(2-\theta)N(\theta)} Y_2(t,I_{FSr-1}) + \tfrac{2\theta}{(2-\theta)N(\theta)} \int_0^t Y_2(\phi,I_{FSr-1})\, d\phi \\
R_{FSr}(t) &= \tfrac{2(1-\theta)}{(2-\theta)N(\theta)} Y_3(t,R_{FSr-1}) + \tfrac{2\theta}{(2-\theta)N(\theta)} \int_0^t Y_3(\phi,R_{FSr-1})\, d\phi \\
S_{FIr}(t) &= \tfrac{2(1-\theta)}{(2-\theta)N(\theta)} Y_4(t,S_{FIr-1}) + \tfrac{2\theta}{(2-\theta)N(\theta)} \int_0^t Y_4(\phi,I_{Tr-1})\, d\phi \\
I_{FIr}(t) &= \tfrac{2(1-\theta)}{(2-\theta)N(\theta)} Y_5(t,I_{FIr-1}) + \tfrac{2\theta}{(2-\theta)N(\theta)} \int_0^t Y_5(\phi,I_{FIr-1})\, d\phi \\
R_{FIr}(t) &= \tfrac{2(1-\theta)}{(2-\theta)N(\theta)} Y_6(t,R_{FIr-1}) + \tfrac{2\theta}{(2-\theta)N(\theta)} \int_0^t Y_6(\phi,R_{FIr-1})\, d\phi \\
S_{Ar}(t) &= \tfrac{2(1-\theta)}{(2-\theta)N(\theta)} Y_5(t,S_{Ar-1}) + \tfrac{2\theta}{(2-\theta)N(\theta)} \int_0^t Y_5(\phi,S_{Ar-1})\, d\phi
\end{aligned}
\right\} \tag{25}
$$

Where $S_{FS0} = S_{FS}(0)$, $I_{FS0} = I_{FS}(0)$, $R_{FS0} = R_{FS}(0)$, $S_{FI0} = S_{FI}(0)$, $I_{FI0} = I_{FI}(0)$, $R_{FI0} = R_{FI}(0)$, $S_{A0} = S_A(0)$, $I_{A0} = I_A(0)$, $R_{A0} = R_A(0)$ are the initial conditions for the recursive expression given in (25).

Equation (26) is obtained after taking the difference between successive terms.

$$
\begin{aligned}
\psi_r(t) &= S_{FSr}(t) - S_{FS(r-1)}(t) = \frac{2(1-\theta)}{(2-\theta)N(\theta)} Y_1\left(t, S_{FS(r-1)}\right) + \frac{2\theta}{(2-\theta)N(\theta)} \int_0^t Y_1\left(\phi, S_{FS(r-1)}\right) d\phi, \\
\chi_r(t) &= I_{FSr}(t) - I_{FS(r-1)}(t) = \frac{2(1-\theta)}{(2-\theta)N(\theta)} Y_2\left(t, I_{FS(r-1)}\right) + \frac{2\theta}{(2-\theta)N(\theta)} \int_0^t Y_2\left(\phi, I_{FS(r-1)}\right) d\phi, \\
\pi_r(t) &= R_{FSr}(t) - R_{FS(r-1)}(t) = \frac{2(1-\theta)}{(2-\theta)N(\theta)} Y_3\left(t, R_{FS(r-1)}\right) + \frac{2\theta}{(2-\theta)N(\theta)} \int_0^t Y_3\left(\phi, R_{FS(r-1)}\right) d\phi, \\
\Omega_r(t) &= S_{FIr}(t) - S_{FI(r-1)}(t) = \frac{2(1-\theta)}{(2-\theta)N(\theta)} Y_4\left(t, S_{FI(r-1)}\right) + \frac{2\theta}{(2-\theta)N(\theta)} \int_0^t Y_4\left(\phi, S_{FI(r-1)}\right) d\phi, \\
\sigma_r(t) &= I_{FIr}(t) - I_{FI(r-1)}(t) = \frac{2(1-\theta)}{(2-\theta)N(\theta)} Y_5\left(t, I_{FI(r-1)}\right) + \frac{2\theta}{(2-\theta)N(\theta)} \int_0^t Y_5\left(\phi, I_{FI(r-1)}\right) d\phi, \\
\Delta_r(t) &= R_{FIr}(t) - R_{FI(r-1)}(t) = \frac{2(1-\theta)}{(2-\theta)N(\theta)} Y_6\left(t, R_{FI(r-1)}\right) + \frac{2\theta}{(2-\theta)N(\theta)} \int_0^t Y_6\left(\phi, R_{FI(r-1)}\right) d\phi, \\
\zeta_r(t) &= S_{Ar}(t) - S_{A(r-1)}(t) = \frac{2(1-\theta)}{(2-\theta)N(\theta)} Y_7\left(t, S_{A(r-1)}\right) + \frac{2\theta}{(2-\theta)N(\theta)} \int_0^t Y_7\left(\phi, S_{A(r-1)}\right) d\phi, \\
\eta_r(t) &= I_{Ar}(t) - I_{A(r-1)}(t) = \frac{2(1-\theta)}{(2-\theta)N(\theta)} Y_8\left(t, I_{A(r-1)}\right) + \frac{2\theta}{(2-\theta)N(\theta)} \int_0^t Y_8\left(\phi, I_{A(r-1)}\right) d\phi, \\
\xi_r(t) &= R_{Ar}(t) - R_{A(r-1)}(t) = \frac{2(1-\theta)}{(2-\theta)N(\theta)} Y_9\left(t, R_{A(r-1)}\right) + \frac{2\theta}{(2-\theta)N(\theta)} \int_0^t Y_9\left(\phi, R_{A(r-1)}\right) d\phi.
\end{aligned} \tag{26}
$$

Expressing our model variables in terms of an infinite series, we have that

$$
\begin{aligned}
&S_{FSr}(t) = \sum_{i=1}^{r} \psi_i(t), \quad I_{FSr}(t) = \sum_{i=1}^{r} \chi_i(t), \quad R_{FSr}(t) = \sum_{i=1}^{r} \pi_i(t), \\
&S_{FIr}(t) = \sum_{i=1}^{r} \Omega_i(t), \quad I_{FIr}(t) = \sum_{i=1}^{r} \sigma_i(t), \quad R_{FIr}(t) = \sum_{i=1}^{r} \Delta_i(t), \\
&S_{Ar}(t) = \sum_{i=1}^{r} \zeta_i(t), \quad I_{Ar}(t) = \sum_{i=1}^{r} \eta_i(t), \quad R_{Ar}(t) = \sum_{i=1}^{r} \xi_i(t).
\end{aligned}
$$

We obtained equation (27) by taking the norm of equation (26).

$$
\begin{aligned}
\|\psi_r(t)\| &= \|S_{FSr}(t) - S_{FSr-1}(t)\| \\
&= \left\| \frac{2(1-\theta)}{(2-\theta)N(\theta)} Y_1(t, S_{FSr-1}) + \frac{2\theta}{(2-\theta)N(\theta)} \int_0^t Y_1(\phi, S_{FSr-1}) d\phi \right\|
\end{aligned} \tag{27}
$$

Equation(27) is modified as (28), when we apply the triangle inequality

$$\begin{aligned}\|\psi_r(t)\| &= \|S_{FSr}(t) - S_{FSr-1}(t)\| \\ &\leq \frac{2(1-\theta)}{(2-\theta)N(\theta)}\|Y_1(t,S_{FSr-1})\| + \frac{2\theta}{(2-\theta)N(\theta)}\left\|\int_0^t Y_1(\phi,S_{FSr-1})d\phi\right\|\end{aligned} \tag{28}$$

Using the Lipschitz condition which was satisfied from theorem (3.1), section (3.2) by kernels, we now rewrite equation (28) as

$$\begin{aligned}\|\psi_r(t)\| &= \|S_{FSr}(t) - S_{FSr-1}(t)\| \\ &\leq \frac{2(1-\theta)}{(2-\theta)N(\theta)}\rho_1\|S_{FSr-1} - S_{FSr-2}\| + \frac{2\theta}{(2-\theta)N(\theta)}\rho_1\int_0^t \|S_{FSr-1} - S_{FSr-2}\|d\phi\end{aligned} \tag{29}$$

Therefore we now have

$$\|\psi_r(t)\| = \|S_{FSr}(t) - S_{FSr-1}(t)\| \leq \frac{2(1-\theta)}{(2-\theta)N(\theta)}\rho_1\|\psi_{r-1}(t)\| + \frac{2\theta}{(2-\theta)N(\theta)}\rho_1\int_0^t \|\psi_{r-1}(t)\|d\phi \tag{30}$$

The following results are obtained following the same procedure used in equation (30)

$$\begin{aligned}
\|\chi_r(t)\| &= \|I_{FSr}(t) - I_{FSr-1}(t)\| \leq \tfrac{2(1-\theta)}{(2-\theta)N(\theta)}\rho_1\|\chi_{r-1}(t)\| + \tfrac{2\theta}{(2-\theta)N(\theta)}\rho_1\int_0^t \|\chi_{r-1}(\phi)\|d\phi \\
\|\pi_r(t)\| &= \|R_{FSr}(t) - R_{FSr-1}(t)\| \leq \tfrac{2(1-\theta)}{(2-\theta)N(\theta)}\rho_2\|\pi_{r-1}(t)\| + \tfrac{2\theta}{(2-\theta)N(\theta)}\rho_2\int_0^t \|\pi_{r-1}(\phi)\|d\phi \\
\|\Omega_r(t)\| &= \|S_{FIr}(t) - S_{FIr-1}(t)\| \leq \tfrac{2(1-\theta)}{(2-\theta)N(\theta)}\rho_3\|\Omega_{r-1}(t)\| + \tfrac{2\theta}{(2-\theta)N(\theta)}\rho_3\int_0^t \|\Omega_{r-1}(\phi)\|d\phi \\
\|\sigma_r(t)\| &= \|I_{FIr}(t) - I_{FIr-1}(t)\| \leq \tfrac{2(1-\theta)}{(2-\theta)N(\theta)}\rho_4\|\sigma_{r-1}(t)\| + \tfrac{2\theta}{(2-\theta)N(\theta)}\rho_4\int_0^t \|\sigma_{r-1}(\phi)\|d\phi \\
\|\Delta_r(t)\| &= \|R_{FIr}(t) - R_{FIr-1}(t)\| \leq \tfrac{2(1-\theta)}{(2-\theta)N(\theta)}\rho_5\|\Delta_{r-1}(t)\| + \tfrac{2\theta}{(2-\theta)N(\theta)}\rho_5\int_0^t \|\Delta_{r-1}(\phi)\|d\phi \\
\|\zeta_r(t)\| &= \|S_{Ar}(t) - S_{Ar-1}(t)\| \leq \tfrac{2(1-\theta)}{(2-\theta)N(\theta)}\rho_6\|\zeta_{r-1}(t)\| + \tfrac{2\theta}{(2-\theta)N(\theta)}\rho_6\int_0^t \|\zeta_{r-1}(\phi)\|d\phi \\
\|\eta_r(t)\| &= \|I_{Ar}(t) - I_{Ar-1}(t)\| \leq \tfrac{2(1-\theta)}{(2-\theta)N(\theta)}\rho_7\|\eta_{r-1}(t)\| + \tfrac{2\theta}{(2-\theta)N(\theta)}\rho_7\int_0^t \|\eta_{r-1}(\phi)\|d\phi \\
\|\xi_r(t)\| &= \|R_{Ar}(t) - R_{Ar-1}(t)\| \leq \tfrac{2(1-\theta)}{(2-\theta)N(\theta)}\rho_8\|\xi_{r-1}(t)\| + \tfrac{2\theta}{(2-\theta)N(\theta)}\rho_8\int_0^t \|\xi_{r-1}(\phi)\|d\phi
\end{aligned} \tag{31}$$

Theorem 3.2. *The fractional order model (9) coupled solution exist, if there exist some t_0 whenever*

$$\frac{2(1-\theta)}{(2-\theta)N(\theta)}\rho_1 + \frac{2\theta}{(2-\theta)}\rho_1 t_0 < 1$$

The model variables $S(t), E(t), Q(t), I(Tt)$ and $R(t)$ are taken to be bounded functions of which Lipschitz condition is fulfilled by their kernels.

We therefore obtained the following results by employing equations (30) and (31) recursively.

$$
\begin{aligned}
\|\psi_r(t)\| &\leq \|S_{FS}(0)\| \left[\tfrac{2(1-\theta)}{(2-\theta)N(\theta)}\rho_1 + \tfrac{2(1-\theta)}{(2-\theta)N(\theta)}\rho_1 t\right]^r \\
\|\chi_r(t)\| &\leq \|I_{FS}(0)\| \left[\tfrac{2(1-\theta)}{(2-\theta)N(\theta)}\rho_2 + \tfrac{2(1-\theta)}{(2-\theta)N(\theta)}\rho_2 t\right]^r \\
\|\pi_r(t)\| &\leq \|R_{FS}(0)\| \left[\tfrac{2(1-\theta)}{(2-\theta)N(\theta)}\rho_3 + \tfrac{2(1-\theta)}{(2-\theta)N(\theta)}\rho_3 t\right]^r \\
\|\Omega_r(t)\| &\leq \|S_{FI}(0)\| \left[\tfrac{2(1-\theta)}{(2-\theta)N(\theta)}\rho_4 + \tfrac{2(1-\theta)}{(2-\theta)N(\theta)}\rho_4 t\right]^r \\
\|\sigma_r(t)\| &\leq \|I_{FI}(0)\| \left[\tfrac{2(1-\theta)}{(2-\theta)N(\theta)}\rho_5 + \tfrac{2(1-\theta)}{(2-\theta)N(\theta)}\rho_5 t\right]^r \\
\|\Delta_r(t)\| &\leq \|R_{FI}(0)\| \left[\tfrac{2(1-\theta)}{(2-\theta)N(\theta)}\rho_6 + \tfrac{2(1-\theta)}{(2-\theta)N(\theta)}\rho_6 t\right]^r \\
\|\zeta_r(t)\| &\leq \|S_A(0)\| \left[\tfrac{2(1-\theta)}{(2-\theta)N(\theta)}\rho_7 + \tfrac{2(1-\theta)}{(2-\theta)N(\theta)}\rho_7 t\right]^r \\
\|\eta_r(t)\| &\leq \|I_A(0)\| \left[\tfrac{2(1-\theta)}{(2-\theta)N(\theta)}\rho_8 + \tfrac{2(1-\theta)}{(2-\theta)N(\theta)}\rho_8 t\right]^r \\
\|\xi_r(t)\| &\leq \|R_A(0)\| \left[\tfrac{2(1-\theta)}{(2-\theta)N(\theta)}\rho_9 + \tfrac{2(1-\theta)}{(2-\theta)N(\theta)}\rho_9 t\right]^r
\end{aligned} \tag{32}
$$

We assume the following so as to show that equation (32) is a unique solution of the Caputo-Fabrizio derivative Monkeypox model presented in equation (10).

$$
\left.
\begin{aligned}
S_{FS}(t) - S_{FS}(0) &= S_{FSr}(t) - A_r(t), \\
I_{FS}(t) - I_{FS}(0) &= I_{FSr}(t) - B_r(t), \\
R_{FS}(t) - R_{FS}(0) &= R_{FSr}(t) - C_r(t), \\
S_{FI}(t) - S_{FI}(0) &= S_{FIr}(t) - D_r(t), \\
I_{FI}(t) - I_{FI}(0) &= I_{FIr}(t) - F_r(t), \\
R_{FI}(t) - R_{FI}(0) &= R_{FIr}(t) - G_r(t), \\
S_A(t) - S_A(0) &= S_{Ar}(t) - H_r(t), \\
I_A(t) - I_A(0) &= I_{Ar}(t) - I_r(t), \\
R_A(t) - R_A(0) &= R_{Ar}(t) - J_r(t)
\end{aligned}
\right\} \tag{33}
$$

So that

$$
\begin{aligned}
\|A_r(t)\| = \Bigg\| &\frac{2(1-\theta)}{(2-\theta)N(\theta)} Y_1(t, S_{FS}) - Y_1(t, S_{r-1}) \\
&+ \frac{2\theta}{(2-\theta)N(\theta)} \int_0^t \left(Y_1(\phi, S_{FS}) - Y_1(\phi, S_{FSr-1})\right) d\phi \Bigg\|
\end{aligned}
$$

$$
\leq \frac{2(1-\theta)}{(2-\theta)N(\theta)} \|Y_1(t, S_{FS}) - Y_1(t, S_{FSr-1})\| + \frac{2\theta}{(2-\theta)N(\theta)} \int_0^t \|Y_1(\phi, S_{FS}) - Y_1(\phi, S_{r-1})\| \, d\phi,
$$

$$
\|A_r(t)\| \leq \frac{2(1-\theta)}{(2-\theta)N(\theta)} \rho_1 \|S_{FS} - S_{FSr-1}\| + \frac{2\theta}{(2-\theta)N(\theta)} \|S_{FS} - S_{FSr-1}\| t. \tag{34}
$$

Then,

$$\|A_r(t)\| \leq \left[\frac{2(1-\theta)}{(2-\theta)N(\theta)}\rho_1 + \frac{2\theta}{(2-\theta)N(\theta)}\rho_1 t\right]^{r+1} I_{FS}. \tag{35}$$

When $t = t_0$, we then have that

$$\|A_r(t)\| \leq \left[\frac{2(1-\theta)}{(2-\theta)N(\theta)}\rho_1 + \frac{2\theta}{(2-\theta)N(\theta)}\rho_1 t_0\right]^{r+1} I_{FS}. \tag{36}$$

Taking the limit of equation (36) as $r \to \inf$, then we have $\|A_r(t)\|^r$ leading to zero.

In the same way, we can show that $\|B_r(t)\| \to 0$, $\|C_r(t)\| \to 0$, $\|D_r(t)\| \to 0$, $\|F_r(t)\| \to 0$, $\|G_r(t)\| \to 0$, $\|H_r(t)\| \to 0$, $\|I_r(t)\| \to 0$, $\|J_r(t)\| \to 0$.

We therefore conclude that the solution to our model (10) exists and proved.

We now discuss the uniqueness of the model (10 solution) in theorem (3.3)

Theorem 3.3. *The fractional Monkeypox model (10) with Caputo-Fabrizio derivative has a unique solution whenever*

$$\left(1 - \frac{2(1-\theta)}{(2-\theta)N(\theta)}\rho_1 - \frac{2\theta}{(2-\theta)N(\theta)}\rho_1 t\right) > 0$$

Assuming that the fractional model (10) has another solution of the form

$S^*_{FS}(t), I^*_{FS}(t), R^*_{FS}(t), S^*_{FI}(t)$, $I^*_{FI}(t)$, $S^*_A(t)$, $I^*_{FI}(t)$, $I^*_A(t)$, therefore

$$S_{FS}(t) - S^*_{FS}(t) = \frac{2(1-\theta)}{(2-\theta)N(\theta)}\left(Y_1(t, S_{FS}) - Y_1(t, S^*_{FS})\right) + \frac{2\theta}{(2-\theta)N(\theta)}\int_0^t \left(Y_1(\phi, S_{FS}) - Y_1(\phi, S^*_{FS})\right) d\phi \tag{37}$$

Taking the norm of the above equation (37), we have

$$\begin{aligned} \|S_{FS}(t) - S^*_{FS}(t)\| \leq{}& \frac{2(1-\theta)}{(2-\theta)N(\theta)} \|(Y_1(t, S_{FS}) - Y_1(t, S^*_{FS}))\| \\ &+ \frac{2\theta}{(2-\theta)N(\theta)} \int_0^t \|(Y_1(\phi, S_{FS}) - Y_1(\phi, S^*_{FS}))\| \, d\phi \end{aligned} \tag{38}$$

Since the Lipschitz condition is satisfied by the kernel, then we have that,

$$\begin{aligned} \|S_{FS}(t) - S^*_{FS}(t)\| \leq{}& \frac{2(1-\theta)}{(2-\theta)N(\theta)}\rho_1 \|S(t) - S^*_{FS}(t)\| \\ &+ \frac{2\theta}{(2-\theta)N(\theta)}\rho_1 t \|S_{FS}(t) - S^*_{FS}(t)\|. \end{aligned} \tag{39}$$

Equation (39) can also be expressed as

$$\|S_{FS}(t)-S^{*}_{FS}(t)\|\left(1-\frac{2(1-\theta)}{(2-\theta)N(\theta)}\rho_1-\frac{\theta}{(2-\theta)N(\theta)}\rho_1 t\right)\leq 0 \tag{40}$$

But

$$\|S_{FS}(t)-S^{*}_{FS}(t)\|=0 \tag{41}$$

Therefore

$$S_{FS}(t)=S^{*}_{FS}(t) \tag{42}$$

This implies the model solution is proved to be unique, the remaining fractions $I_{FS}(t), R_{FS}(t), S_{FS}(t)$, $S_A(t)$, $I_A(t)$ and $R_A(t)$ results can be obtained following the same procedure.

3.3. Caputo-Fabrizio derivative numerical algorithm. In this section, we discussed a numerical method for Caputo-Fabrizio fractional order derivative following the method used in [34].

$${}^{CF}_{0}D^{\theta}_{t}x(t)=y(t,x(t)) \tag{43}$$

Using the calculus fundamental theorem we now have,

$$x(t)-x(0)=\frac{1-\theta}{N(\theta)}y(t,x(t))+\frac{\theta}{N(\theta)}\int_0^t y(\psi,x(\psi))d\psi \tag{44}$$

For a general case (44) becomes

$$x(t_{r+1})-x(0)=\frac{1-\theta}{N(\theta)}y(t_{r+1},x(t_{r+1}))+\frac{\theta}{N(\theta)}\int_0^{t_{r+1}} y(t,x(t))dt \tag{45}$$

Secondly,

$$x(t_r)-x(0)=\frac{1-\theta}{N(\theta)}y(t_{r-1},x(t_{r-1}))+\frac{\theta}{N(\theta)}\int_0^{t_r} y(t,x(t))dt \tag{46}$$

From (46), we have that

$$x(t_{r+1})-x(t_r)=\frac{(1-\theta)}{N(\theta)}\left(y(t_r,x(t_r))-y(t_{r-1},x(t_{r-1}))+\frac{\theta}{N(\theta)}\int_{t_r}^{t_{r+1}} y(t,x(t))\,dt,\right. \tag{47}$$

Where

$$\begin{aligned}(48)\qquad &\int_{t_r}^{t_{r+1}} y(t,x(t))\,dt = \int_{t_r}^{t_{r+1}} \left[\frac{y(t_r,x_r)}{p}(t-t_{r-1}) - \frac{y(t_{r-1},x_{r-1})}{p}(t-t_r)\right] \\ &= \frac{3P}{2}y(t_r,x_n) - \frac{P}{2}y(t_{r-1},x_{r-1}),\end{aligned}$$

From equation (47), the following solution is obtained.

$$\begin{aligned}(49)\qquad &x(t_{r+1}) - x(t_r) = \frac{(1-\theta)}{N(\theta)}\left[(y(t_r,x(t_r)) - y(t_{r-1},x(t_{r-1}))\right] \\ &+\frac{\theta}{N(\theta)}\left[\frac{3P}{2}y(t_r,x(t_r)) - \frac{P}{2}y(t_{r-1},x(t_{r-1}))\right]\end{aligned}$$

Therefore,

$$\begin{aligned}(50)\qquad &x(t_{r+1}) - x(t_r) = \left(\frac{(1-\theta)}{N(\theta)} + \frac{3\theta P}{2N(\theta)}\right)y(t_r,x(t_r)) \\ &-\left(\frac{(1-\theta)}{N(\theta)} + \frac{\theta P}{2N(\theta)}\right)y(t_{r-1},x(t_{r-1}))\end{aligned}$$

Equation (50) has the solution of the form

$$\begin{aligned}(51)\qquad &x(_{r+1}) - x(_r) = \left(\frac{(1-\theta)}{N(\theta)} + \frac{3\theta P}{2N(\theta)}\right)y(_r,x(t_r)) \\ &-\left(\frac{(1-\theta)}{N(\theta)} + \frac{\theta P}{2N(\theta)}\right)y(t_{r-1},x(t_{r-1}))\end{aligned}$$

This is the two step Adams-Bashforth-Moulton numerical method for the Caputo-Fabrizio fractional order derivative.

3.4. Caputo-Fabrizio Derivative Monkeypox Model Numerical Method. We now employ the above two step Adams-Bashforth-Moulton numerical algorithm proposed to obtain the approximate solution of model (10).

$$\begin{aligned}(52)\qquad &S_{FSr+1} = S_{FSr} + \left(\frac{(1-\theta)}{N(\theta)} + \frac{3\theta P}{2N(\theta)}\right)y_1(t_r,S_{FSr},I_{FSr},R_{FSr},S_{FIr},I_{FIr},R_{FIr},S_{Ar},I_{Ar},R_{Ar}) \\ &-\left(\frac{(1-\theta)}{N(\theta)} + \frac{\theta P}{2N(\theta)}\right)y_1(t_{r-1},S_{FSr-1},I_{FSr-1},R_{FSr-1},S_{FIr-1},I_{FIr-1},R_{FIr-1},S_{Ar-1},I_{Ar-1},R_{Ar-1}), \\ &I_{FSr+1} = I_{FSr} + \left(\frac{(1-\theta)}{N(\theta)} + \frac{3\theta P}{2N(\theta)}\right)y_2(t_r,S_{FSr},I_{FSr},R_{FSr},S_{FIr},I_{FIr},R_{FIr},S_{Ar},I_{Ar},R_{Ar}) \\ &-\left(\frac{(1-\theta)}{N(\theta)} + \frac{\theta P}{2N(\theta)}\right)y_2(t_{r-1},S_{FSr-1},I_{FSr-1},R_{FSr-1},S_{FIr-1},I_{FIr-1},R_{FIr-1},S_{Ar-1},I_{Ar-1},R_{Ar-1}), \\ &R_{FSr+1} = R_{FSr} + \left(\frac{(1-\theta)}{N(\theta)} + \frac{3\theta P}{2N(\theta)}\right)y_3(t_r,S_{FSr},I_{FSr},R_{FSr},S_{FIr},I_{FIr},R_{FIr},S_{Ar},I_{Ar},R_{Ar}) \\ &-\left(\frac{(1-\theta)}{N(\theta)} + \frac{\theta P}{2N(\theta)}\right)y_3(t_{r-1},S_{FSr-1},I_{FSr-1},R_{FSr-1},S_{FIr-1},I_{FIr-1},R_{FIr-1},S_{Ar-1},I_{Ar-1},R_{Ar-1}) \\ &S_{FIr+1} = S_{FIr} + \left(\frac{(1-\theta)}{N(\theta)} + \frac{3\theta P}{2N(\theta)}\right)y_4(t_r,S_{FSr},I_{FSr},R_{FSr},S_{FIr},I_{FIr},R_{FIr},S_{Ar},I_{Ar},R_{Ar}) \\ &-\left(\frac{(1-\theta)}{N(\theta)} + \frac{\theta P}{2N(\theta)}\right)y_4(t_{r-1},S_{FSr-1},I_{FSr-1},R_{FSr-1},S_{FIr-1},I_{FIr-1},R_{FIr-1},S_{Ar-1},I_{Ar-1},R_{Ar-1}), \\ &I_{FIr+1} = I_{FIr} + \left(\frac{(1-\theta)}{N(\theta)} + \frac{3\theta P}{2N(\theta)}\right)y_5(t_r,S_{FSr},I_{FSr},R_{FSr},S_{FIr},I_{FIr},R_{FIr},S_{Ar},I_{Ar},R_{Ar}) \\ &-\left(\frac{(1-\theta)}{N(\theta)} + \frac{\theta P}{2N(\theta)}\right)y_5(t_{r-1},S_{FSr-1},I_{FSr-1},R_{FSr-1},S_{FIr-1},I_{FIr-1},R_{FIr-1},S_{Ar-1},I_{Ar-1},R_{Ar-1}), \\ &R_{FIr+1} = R_{FIr} + \left(\frac{(1-\theta)}{N(\theta)} + \frac{3\theta P}{2N(\theta)}\right)y_6(t_r,S_{FSr},I_{FSr},R_{FSr},S_{FIr},I_{FIr},R_{FIr},S_{Ar},I_{Ar},R_{Ar})\end{aligned}$$

$$-\left(\frac{(1-\theta)}{N(\theta)}+\frac{\theta P}{2N(\theta)}\right)y_6\left(t_{r-1},S_{FSr-1},I_{FSr-1},R_{FSr-1},S_{FIr-1},I_{FIr-1},R_{FIr-1},S_{Ar-1},I_{Ar-1},R_{Ar-1}\right)$$

4. Adams-type Predictor Corrector Numerical Method with Atagana-Baleanu-derivative fractional order Model

In this section, we employ the Adams-type predictor corrector numerical method used [42] to obtain an approximate solution of our Monkeypox model (11).

Recall that our Monkeypox model in the sense of Atagana-Baleanu-derivative with the generalized Mittag-Leffler function is given as:

$$\left.\begin{aligned}
&{}_0^{ABC}D_t^{\theta}S_{FS}(t)=a\Lambda_S-\tfrac{m(\alpha_1I_{FS}+\alpha_2I_{FI}+\alpha_3I_A)}{N_{FS}}S_{FS}-\mu_HS_{FS},\\
&{}_0^{ABC}D_t^{\theta}I_{FS}(t)=\tfrac{m(\alpha_1I_{FS}+\alpha_2I_{FI}+\alpha_3I_A)}{N_{FS}}S_{FS}-(\tau_S+\delta_S+\mu_H)I_{FS},\\
&{}_0^{ABC}D_t^{\theta}R_{FS}(t)=\tau_SI_{FS}-\mu_HR_{FS},\\
&{}_0^{ABC}D_t^{\theta}S_{FI}(t)=(1-a)\Lambda_S-\tfrac{(\alpha_4I_{FS}+\alpha_5I_{FI}+\alpha_6I_A)}{N_{FI}}S_{FI}-\mu_HS_{FI},\\
&{}_0^{ABC}D_t^{\theta}I_{FI}(t)=\tfrac{\alpha_4I_{FS}+\alpha_5I_{FI}+\alpha_6I_A}{N_{FI}}S_{FI}-(\tau_I+\delta_I+\mu_H)I_{FI},\\
&{}_0^{ABC}D_t^{\theta}R_{FI}(t)=\tau_II_{FI}-\mu_HR_{FI},\\
&{}_0^{ABC}D_t^{\theta}S_A(t)=\Lambda_A-\tfrac{\alpha_7I_A}{N_A}S_A-\mu_AS_A,\\
&{}_0^{ABC}D_t^{\theta}I_A(t)=\tfrac{\alpha_7I_A}{N_A}S_A-(\tau_A+\delta_A+\mu_A)I_A,\\
&{}_0^{ABC}D_t^{\theta}R_A(t)=\tau_AI_A-\mu_AR_A.
\end{aligned}\right\}$$

This can also be written as:

$$\left.\begin{aligned}
&{}_0^{ABC}D_t^{\theta}S_{FS}(t)=y_1\left(t,S_{FS},I_{FS},R_{FS},S_{FI},I_{FI},R_{FI},S_A,I_A,R_A\right),\\
&{}_0^{ABC}D_t^{\theta}I_{FS}(t)=y_2\left(t,S_{FS},I_{FS},R_{FS},S_{FI},I_{FI},R_{FI},S_A,I_A,R_A\right),\\
&{}_0^{ABC}D_t^{\theta}R_{FS}(t)=y_3\left(t,S_{FS},I_{FS},R_{FS},S_{FI},I_{FI},R_{FI},S_A,I_A,R_A\right),\\
&{}_0^{ABC}D_t^{\theta}S_{FI}(t)=y_4\left(t,S_{FS},I_{FS},R_{FS},S_{FI},I_{FI},R_{FI},S_A,I_A,R_A\right),\\
&{}_0^{ABC}D_t^{\theta}I_{FI}(t)=y_5\left(t,S_{FS},I_{FS},R_{FS},S_{FI},I_{FI},R_{FI},S_A,I_A,R_A\right),\\
&{}_0^{ABC}D_t^{\theta}R_{FI}(t)=y_6\left(t,S_{FS},I_{FS},R_{FS},S_{FI},I_{FI},R_{FI},S_A,I_A,R_A\right),\\
&{}_0^{ABC}D_t^{\theta}S_A(t)=y_7\left(t,S_{FS},I_{FS},R_{FS},S_{FI},I_{FI},R_{FI},S_A,I_A,R_A\right),\\
&{}_0^{ABC}D_t^{\theta}I_A(t)=y_8\left(t,S_{FS},I_{FS},R_{FS},S_{FI},I_{FI},R_{FI},S_A,I_A,R_A\right),\\
&{}_0^{ABC}D_t^{\theta}R_A(t)=y_9\left(t,S_{FS},I_{FS},R_{FS},S_{FI},I_{FI},R_{FI},S_A,I_A,R_A\right).
\end{aligned}\right\}\tag{53}$$

Applying the Atagana-Baleanu (AB) fractional order integral on both sides of the equation.

$$
\begin{aligned}
&S_{FS}(t) = S_{FS0}(t) + \tfrac{(1-\theta)}{AB(\theta)} y_1(t, S_{FS}, I_{FS}, R_{FS}, S_{FI}, I_{FI}, R_{FI}, S_A, I_A, R_A) + \\
&\tfrac{\theta}{AB(\theta)} \int_0^t y_1(t, S_{FS}, I_{FS}, R_{FS}, S_{FI}, I_{FI}, R_{FI}, S_A, I_A, R_A)(t-\psi)^{\theta-1} d\psi, \\
&I_{FS}(t) = I_{FS0}(t) + \tfrac{(1-\theta)}{AB(\theta)} y_2(t, S_{FS}, I_{FS}, R_{FS}, S_{FI}, I_{FI}, R_{FI}, S_A, I_A, R_A) + \\
&\tfrac{\theta}{AB(\theta)} \int_0^t y_2(t, S_{FS}, I_{FS}, R_{FS}, S_{FI}, I_{FI}, R_{FI}, S_A, I_A, R_A)(t-\psi)^{\theta-1} d\psi, \\
&R_{FS}(t) = R_{FS0}(t) + \tfrac{(1-\theta)}{AB(\theta)} y_3(t, S_{FS}, I_{FS}, R_{FS}, S_{FI}, I_{FI}, R_{FI}, S_A, I_A, R_A) + \\
&\tfrac{\theta}{AB(\theta)} \int_0^t y_3(t, S_{FS}, I_{FS}, R_{FS}, S_{FI}, I_{FI}, R_{FI}, S_A, I_A, R_A)(t-\psi)^{\theta-1} d\psi, \\
&S_{FI}(t) = S_{FI0}(t) + \tfrac{(1-\theta)}{AB(\theta)} y_4(t, S_{FS}, I_{FS}, R_{FS}, S_{FI}, I_{FI}, R_{FI}, S_A, I_A, R_A) + \\
&\tfrac{\theta}{AB(\theta)} \int_0^t y_4(t, S_{FS}, I_{FS}, R_{FS}, S_{FI}, I_{FI}, R_{FI}, S_A, I_A, R_A)(t-\psi)^{\theta-1} d\psi, \\
&I_{FI}(t) = I_{FI0}(t) + \tfrac{(1-\theta)}{AB(\theta)} y_5(t, S_{FS}, I_{FS}, R_{FS}, S_{FI}, I_{FI}, R_{FI}, S_A, I_A, R_A) + \\
&\tfrac{\theta}{AB(\theta)} \int_0^t y_5(t, S_{FS}, I_{FS}, R_{FS}, S_{FI}, I_{FI}, R_{FI}, S_A, I_A, R_A)(t-\psi)^{\theta-1} d\psi, \\
&R_{FI}(t) = R_{FI0}(t) + \tfrac{(1-\theta)}{AB(\theta)} y_6(t, S_{FS}, I_{FS}, R_{FS}, S_{FI}, I_{FI}, R_{FI}, S_A, I_A, R_A) + \\
&\tfrac{\theta}{AB(\theta)} \int_0^t y_6(t, S_{FS}, I_{FS}, R_{FS}, S_{FI}, I_{FI}, R_{FI}, S_A, I_A, R_A)(t-\psi)^{\theta-1} d\psi, \\
&S_A(t) = S_{A0}(t) + \tfrac{(1-\theta)}{AB(\theta)} y_7(t, S_{FS}, I_{FS}, R_{FS}, S_{FI}, I_{FI}, R_{FI}, S_A, I_A, R_A) + \\
&\tfrac{\theta}{AB(\theta)} \int_0^t y_7(t, S_{FS}, I_{FS}, R_{FS}, S_{FI}, I_{FI}, R_{FI}, S_A, I_A, R_A)(t-\psi)^{\theta-1} d\psi, \\
&I_A(t) = I_{A0}(t) + \tfrac{(1-\theta)}{AB(\theta)} y_8(t, S_{FS}, I_{FS}, R_{FS}, S_{FI}, I_{FI}, R_{FI}, S_A, I_A, R_A) + \\
&\tfrac{\theta}{AB(\theta)} \int_0^t y_8(t, S_{FS}, I_{FS}, R_{FS}, S_{FI}, I_{FI}, R_{FI}, S_A, I_A, R_A)(t-\psi)^{\theta-1} d\psi, \\
&R_A(t) = R_{A0}(t) + \tfrac{(1-\theta)}{AB(\theta)} y_9(t, S_{FS}, I_{FS}, R_{FS}, S_{FI}, I_{FI}, R_{FI}, S_A, I_A, R_A) + \\
&\tfrac{\theta}{AB(\theta)} \int_0^t y_9(t, S_{FS}, I_{FS}, R_{FS}, S_{FI}, I_{FI}, R_{FI}, S_A, I_A, R_A)(t-\psi)^{\theta-1} d\psi.
\end{aligned} \tag{54}
$$

To investigate the above fractional order integral numerically, we therefore approximate the fractional order integral numerically. Employing the Adams-type predictor-corrector method presented in [42] for Atagana-Baleanu fractional integral, we now have

$$
{}_0^{AB}I_t^{\theta}\left[x(t)\right] = \frac{1-\theta}{AB(\theta)} x(t) + \frac{\theta}{AB(\theta)\left|\overline{(\theta)}\right.} \int_0^t x(\psi)\,(t-\psi)^{\theta-1} d\psi \tag{55}
$$

By letting $P = \frac{T}{N}, t_r = rp, (r = 0, 1, 2, 3, ...9)$.

We therefore consider the solution in the interval of $[0, T]$.

Therefore the corrector formula for the Atagana-Baleanu fractional-integral version is presented as:

$$x_p(t_{r+1}) = x_0(t_{r+1}) + \frac{(1-\theta)P^\theta}{AB(\theta)\left|(\theta+2)\right.} y\left(t_{r+1}, x_p^V(t_{r+1})\right) + \frac{\theta P^\theta}{AB(\theta)\left|(\theta+2)\right.} \sum_{i=0}^{k} \Upsilon_{i,r+1} y(t_i, x_p(t_i))$$

Where,

$$\Upsilon_{i,r+1} = \begin{cases} r^{\theta+1} - (r-\theta)(r+1)^\theta, if i = 0 \\ (r-i+2)^{\theta+1} + (r-i)^{\theta+1} - 2(r-i+1)^{\theta+1}, 1 \le i \le r, \\ 1 i = r+1 \end{cases}$$

Similarly, the predictor $x^V(t_{r+1})$ is expressed as given below:

$$x_P^V(t_{r+1}) = x_0 + \frac{(1-\theta)}{AB(\theta)} y(t_r, x_P(t_r)) + \frac{\theta}{AB(\theta)\left|(\theta)^2\right.} \sum_{i=0}^{k} \Delta_{i,r+1} y(t_i, x_p(t_i)),$$

Where,

$$\Delta_{i,r+1} = \frac{P^\theta}{\theta}\left((r+1-i)^\theta - (r-i)^\theta\right), 0 \le i \le r$$

We therefore present our model (11) as given in (56) using the Adam-type predictor-corrector numerical method.

$$\begin{aligned}
S_{r+1} &= S(0) + \tfrac{(1-\theta)P^\theta}{AB(\theta)\left|(\theta+2)\right|}\left[y_1(t_{r+1}, S_{r+1}^{FI}, I_{r+1}^{FI}, R_{r+1}^{FI}, S_{r+1}^{FS}, I_{r+1}^{FS}, R_{r+1}^{FS}, S_{r+1}^{A}, I_{r+1}^{A}, R_{r+1}^{A}) \right. \\
&\quad \left. + \tfrac{\theta P^\theta}{AB(\theta)\left|(\theta+2)\right|} \textstyle\sum_{i=0}^{k} \Upsilon_{i,r+1} y_1(t_i, S_i, I_i, R_i, S_A, I_A, R_A)\right], \\
I_{r+1} &= I(0) + \tfrac{(1-\theta)P^\theta}{AB(\theta)\left|(\theta+2)\right|}\left[y_2(t_{r+1}, S_{r+1}^{FI}, I_{r+1}^{FI}, R_{r+1}^{FI}, S_{r+1}^{FS}, I_{r+1}^{FS}, R_{r+1}^{FS}, S_{r+1}^{A}, I_{r+1}^{A}, R_{r+1}^{A}) \right. \\
&\quad \left. + \tfrac{\theta P^\theta}{AB(\theta)\left|(\theta+2)\right|} \textstyle\sum_{i=0}^{k} \Upsilon_{i,r+1} y_1(t_i, S_i, I_i, R_i, S_A, I_A, R_A)\right], \\
R_{r+1} &= R(0) + \tfrac{(1-\theta)P^\theta}{AB(\theta)\left|(\theta+2)\right|}\left[y_3(t_{r+1}, S_{r+1}^{FI}, I_{r+1}^{FI}, R_{r+1}^{FI}, S_{r+1}^{FS}, I_{r+1}^{FS}, R_{r+1}^{FS}, S_{r+1}^{A}, I_{r+1}^{A}, R_{r+1}^{A}) \right. \\
&\quad \left. + \tfrac{\theta P^\theta}{AB(\theta)\left|(\theta+2)\right|} \textstyle\sum_{i=0}^{k} \Upsilon_{i,r+1} y_1(t_i, S_i, I_i, R_i, S_A, I_A, R_A)\right], \\
S_{FI} &= S_{FI}(0) + \tfrac{(1-\theta)P^\theta}{AB(\theta)\left|(\theta+2)\right|}\left[y_4(t_{r+1}, S_{r+1}^{FI}, I_{r+1}^{FI}, R_{r+1}^{FI}, S_{r+1}^{FS}, I_{r+1}^{FS}, R_{r+1}^{FS}, S_{r+1}^{A}, I_{r+1}^{A}, R_{r+1}^{A}) \right. \\
&\quad \left. + \tfrac{\theta P^\theta}{AB(\theta)\left|(\theta+2)\right|} \textstyle\sum_{i=0}^{k} \Upsilon_{i,r+1} y_1(t_i, S_i, I_i, R_i, S_A, I_A, R_A)\right], \\
I_{FI} &= I_{FI}(0) + \tfrac{(1-\theta)P^\theta}{AB(\theta)\left|(\theta+2)\right|}\left[y_5(t_{r+1}, S_{r+1}^{FI}, I_{r+1}^{FI}, R_{r+1}^{FI}, S_{r+1}^{FS}, I_{r+1}^{FS}, R_{r+1}^{FS}, S_{r+1}^{A}, I_{r+1}^{A}, R_{r+1}^{A}) \right. \\
&\quad \left. + \tfrac{\theta P^\theta}{AB(\theta)\left|(\theta+2)\right|} \textstyle\sum_{i=0}^{k} \Upsilon_{i,r+1} y_1(t_i, S_i, I_i, R_i, S_A, I_A, R_A)\right], \\
R_{FI} &= R_{FI}(0) + \tfrac{(1-\theta)P^\theta}{AB(\theta)\left|(\theta+2)\right|}\left[y_6(t_{r+1}, S_{r+1}^{FI}, I_{r+1}^{FI}, R_{r+1}^{FI}, S_{r+1}^{FS}, I_{r+1}^{FS}, R_{r+1}^{FS}, S_{r+1}^{A}, I_{r+1}^{A}, R_{r+1}^{A}) \right. \\
&\quad \left. + \tfrac{\theta P^\theta}{AB(\theta)\left|(\theta+2)\right|} \textstyle\sum_{i=0}^{k} \Upsilon_{i,r+1} y_1(t_i, S_i, I_i, R_i, S_A, I_A, R_A)\right],
\end{aligned} \tag{56}$$

$$
\begin{aligned}
S_A &= S_A(0) + \tfrac{(1-\theta)P^{\theta}}{AB(\theta)\left|\overline{(\theta+2)}\right|}\left[y_7(t_{r+1}, S^{FI}_{r+1}, I^{FI}_{r+1}, R^{FI}_{r+1}, S^{FS}_{r+1}, I^{FS}_{r+1}, R^{FS}_{r+1}, S^{A}_{r+1}, I^{A}_{r+1}, R^{A}_{r+1})\right.\\
&\quad \left. + \tfrac{\theta P^{\theta}}{AB(\theta)\left|\overline{(\theta+2)}\right|}\sum_{i=0}^{k}\Upsilon_{i,r+1}y_1(t_i, S_i, I_i, R_i, S_A, I_A, R_A)\right],\\
I_A &= I_A(0) + \tfrac{(1-\theta)P^{\theta}}{AB(\theta)\left|\overline{(\theta+2)}\right|}\left[y_8(t_{r+1}, S^{FI}_{r+1}, I^{FI}_{r+1}, R^{FI}_{r+1}, S^{FS}_{r+1}, I^{FS}_{r+1}, R^{FS}_{r+1}, S^{A}_{r+1}, I^{A}_{r+1}, R^{A}_{r+1})\right.\\
&\quad \left. + \tfrac{\theta P^{\theta}}{AB(\theta)\left|\overline{(\theta+2)}\right|}\sum_{i=0}^{k}\Upsilon_{i,r+1}y_1(t_i, S_i, I_i, R_i, S_A, I_A, R_A)\right],\\
R_A &= R_A(0) + \tfrac{(1-\theta)P^{\theta}}{AB(\theta)\left|\overline{(\theta+2)}\right|}\left[y_9(t_{r+1}, S^{FI}_{r+1}, I^{FI}_{r+1}, R^{FI}_{r+1}, S^{FS}_{r+1}, I^{FS}_{r+1}, R^{FS}_{r+1}, S^{A}_{r+1}, I^{A}_{r+1}, R^{A}_{r+1})\right.\\
&\quad \left. + \tfrac{\theta P^{\theta}}{AB(\theta)\left|\overline{(\theta+2)}\right|}\sum_{i=0}^{k}\Upsilon_{i,r+1}y_1(t_i, S_i, I_i, R_i, S_A, I_A, R_A)\right].
\end{aligned}
$$

Where $S^{FI}_{r+1}, I^{FI}_{r+1}, R^{FI}_{r+1}, S^{FS}_{r+1}, I^{FS}_{r+1}, R^{FS}_{r+1}, S^{A}_{r+1}, I^{A}_{r+1}, R^{A}_{r+1}$ are the predictors given as:

$$
\begin{aligned}
S_{FSr+1} &= S_{FS}(0) + \frac{(1-\theta)}{AB(\theta)}y_1(t_r, S_{FSr}, I_{FSr}, R_{FSr}, S_{FIr}, I_{FIr}, R_{FIr}, S_{Ar}, I_{Ar}, R_{Ar})\\
&\quad + \frac{\theta}{\left|\overline{(\theta)}\right|^2 AB(\theta)}\sum_{i=0}^{k}\Delta_{i,k+1}y_1(t_i, S_{FSi}, I_{FSi}, R_{FSi}, S_{FIi}, I_{FIi}, R_{FIi}, S_{Ai}, I_{Ai}, R_{Ai}),\\
I_{FSr+1} &= I_{FS}(0) + \frac{(1-\theta)}{AB(\theta)}y_2(t_r, S_{FSr}, I_{FSr}, R_{FSr}, S_{FIr}, I_{FIr}, R_{FIr}, S_{Ar}, I_{Ar}, R_{Ar})\\
&\quad + \frac{\theta}{\left|\overline{(\theta)}\right|^2 AB(\theta)}\sum_{i=0}^{k}\Delta_{i,k+1}y_2(t_i, S_{FSi}, I_{FSi}, R_{FSi}, S_{FIi}, I_{FIi}, R_{FIi}, S_{Ai}, I_{Ai}, R_{Ai}),\\
R_{FSr+1} &= R_{FS}(0) + \frac{(1-\theta)}{AB(\theta)}y_3(t_r, S_{FSr}, I_{FSr}, R_{FSr}, S_{FIr}, I_{FIr}, R_{FIr}, S_{Ar}, I_{Ar}, R_{Ar})\\
&\quad + \frac{\theta}{\left|\overline{(\theta)}\right|^2 AB(\theta)}\sum_{i=0}^{k}\Delta_{i,k+1}y_3(t_i, S_{FSi}, I_{FSi}, R_{FSi}, S_{FIi}, I_{FIi}, R_{FIi}, S_{Ai}, I_{Ai}, R_{Ai}),\\
S_{FIr+1} &= S_{FI}(0) + \frac{(1-\theta)}{AB(\theta)}y_4(t_r, S_{FSr}, I_{FSr}, R_{FSr}, S_{FIr}, I_{FIr}, R_{FIr}, S_{Ar}, I_{Ar}, R_{Ar})\\
&\quad + \frac{\theta}{\left|\overline{(\theta)}\right|^2 AB(\theta)}\sum_{i=0}^{k}\Delta_{i,k+1}y_4(t_i, S_{FSi}, I_{FSi}, R_{FSi}, S_{FIi}, I_{FIi}, R_{FIi}, S_{Ai}, I_{Ai}, R_{Ai}),\\
I_{FIr+1} &= I_{FI}(0) + \frac{(1-\theta)}{AB(\theta)}y_5(t_r, S_{FSr}, I_{FSr}, R_{FSr}, S_{FIr}, I_{FIr}, R_{FIr}, S_{Ar}, I_{Ar}, R_{Ar})\\
&\quad + \frac{\theta}{\left|\overline{(\theta)}\right|^2 AB(\theta)}\sum_{i=0}^{k}\Delta_{i,k+1}y_5(t_i, S_{FSi}, I_{FSi}, R_{FSi}, S_{FIi}, I_{FIi}, R_{FIi}, S_{Ai}, I_{Ai}, R_{Ai}),\\
R_{FIr+1} &= R_{FI}(0) + \frac{(1-\theta)}{AB(\theta)}y_6(t_r, S_{FSr}, I_{FSr}, R_{FSr}, S_{FIr}, I_{FIr}, R_{FIr}, S_{Ar}, I_{Ar}, R_{Ar})
\end{aligned}
\tag{57}
$$

$$+\frac{\theta}{\left|\overline{(\theta)}\right|^2 AB(\theta)}\sum_{i=0}^{k}\Delta_{i,k+1}y_6\left(t_i,S_{FSi},I_{FSi},R_{FSi},S_{FIi},I_{FIi},R_{FIi},S_{Ai},I_{Ai},R_{Ai}\right),$$

$$S_{Ar+1}=S_A(0)+\frac{(1-\theta)}{AB(\theta)}y_7\left(t_r,S_{FSr},I_{FSr},R_{FSr},S_{FIr},I_{FIr},R_{FIr},S_{Ar},I_{Ar},R_{Ar}\right)$$

$$+\frac{\theta}{\left|\overline{(\theta)}\right|^2 AB(\theta)}\sum_{i=0}^{k}\Delta_{i,k+1}y_7\left(t_i,S_{FSi},I_{FSi},R_{FSi},S_{FIi},I_{FIi},R_{FIi},S_{Ai},I_{Ai},R_{Ai}\right)$$

4.1. Fractional Order Monkeypox Model Simulation. In this section, we present the numerical simulation of the Monkeypox (6) model employing the three(3) differential operators used. The values of our model variable(parameters) used for this simulation is presented in Tables (1 and 2) below.

TABLE 1. Variables and Parameters of the Monkeypox Model

Symbol	Description	Values	Source
S_{FS}	Susceptible individuals with food security	200,000,000	[43]
I_{FS}	Infected individuals with food security	10,000,000	Estimated
R_{FS}	Recovered with food security	5,000,000	Estimated
S_{FI}	Susceptible individuals with food insecurity	23,000,000	[43]
I_{FI}	Infected individuals with food insecurity	4,000,000	Estimated
R_{FI}	Recovered individuals with food insecurity	2,000,000	Estimated
S_A	Susceptible animal	10,000	Estimated
I_A	Infected animals	5,000	Estimated
R_A	Recovered animals	3,000	Estimated
Λ_S	Recruitment rate of humans	0.029	[45]
a	Fraction of human recruitment into the food-secure population	0.6	Estimated
m	Modification parameter accounting for the reduced rate of disease contraction in the food-secure population	0.1	Estimated
$\alpha_1,\alpha_2,\alpha_3$	Rates of contact between susceptible food-secure humans and food-secure infected humans, food-insecure infected humans, and infected animals, respectively	0.1, 0.21, 0.00025	[44], Estimated, [45]

TABLE 2. Variables and Parameters of the Monkeypox Model

Symbol	Description	Values	Source
$\alpha_4, \alpha_5, \alpha_6$	Rates of contact between susceptible food-insecure humans and food-secure infected humans, food-insecure infected humans, and infected animals, respectively	0.36, 0.17, 0.32	Estimated Estimated, Estimated
α_7	Rate of contact between susceptible animals and infected animals	0.3412	[44]
τ_S, τ_I, τ_A	Recovery rates of infected food-secure humans, infected food insecure humans and infected animals respectively	0.079, 0.21, 0.11	[44] Estimated, Estimated
$\delta_S, \delta_I, \delta_A$	Disease-induced death rates of infected food-secure humans, infected food insecure humans and infected animals	0.1001, 0.26, 0.5	[46], Estimated, [47]
μ_H	Natural death rate for humans	0.00303	[47]
μ_A	Natural death rate for animals	0.002	[47]

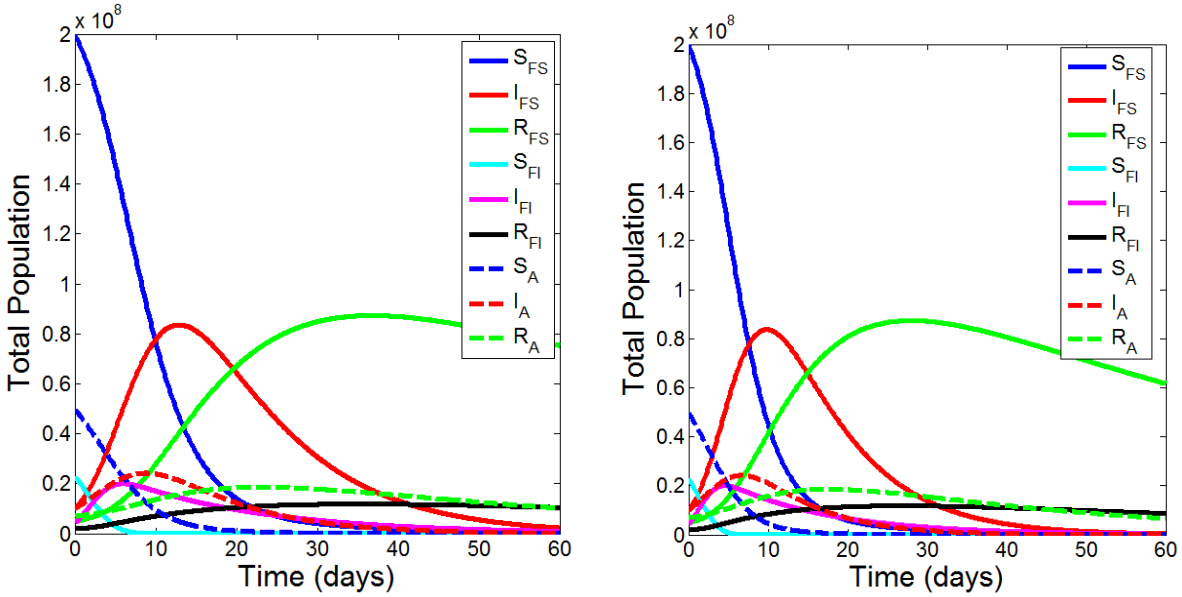

(A) **Behaviors of the system (9) by adopting Caputo derivative for $\theta = 0.95$**

(B) **Behaviors of the system (9) by adopting Caputo derivative for $\theta = 0.85$**

FIGURE 2. **Total Human Population**

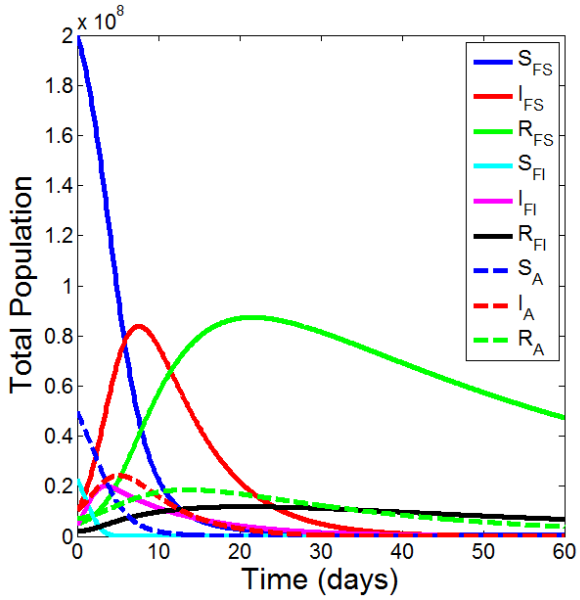

(A) **Behaviors of the system (9) by adopting Caputo derivative for $\theta = 0.75$**

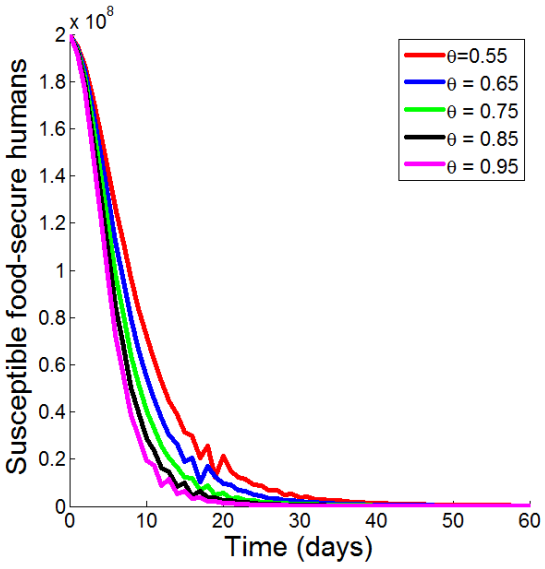

(B) **The plot for the Susceptible food-secure humans for Caputo derivative**

FIGURE 3. **Human Population**

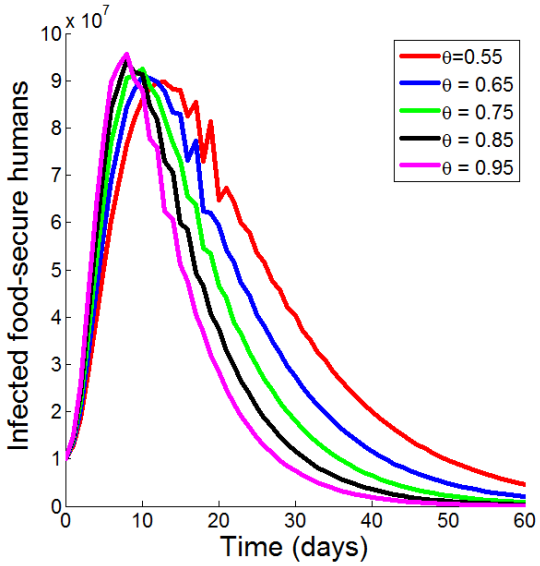

(A) **The plot for the Infected food-secure humans for Caputo derivative**

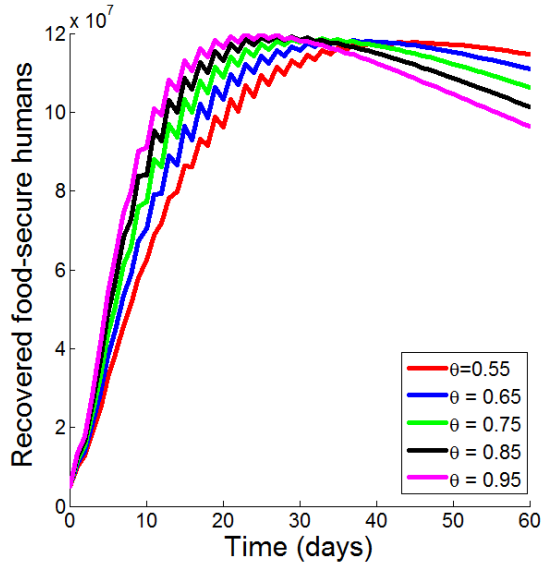

(B) **The plot for the Recovered food-secure humans for Caputo derivative**

FIGURE 4. **Human Population**

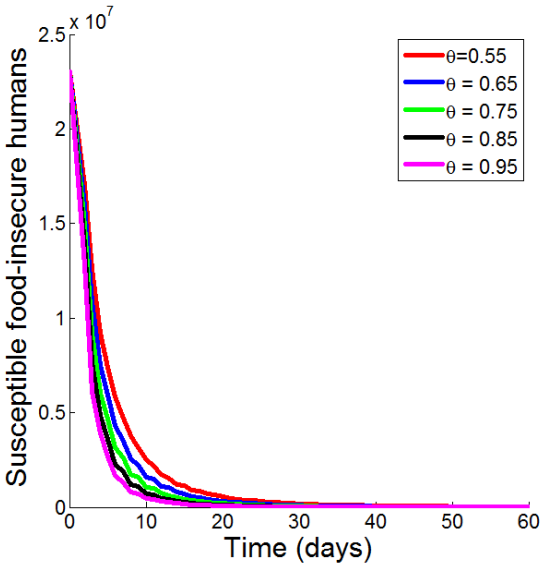

(A) **The plot for the susceptible food-insecure humans for Caputo derivative**

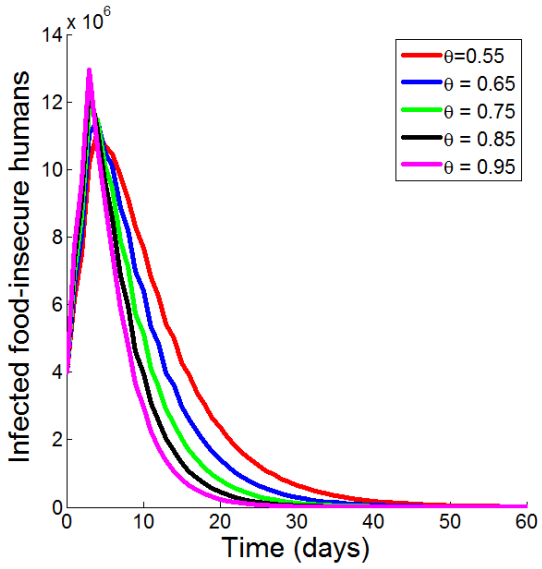

(B) **The plot for the infected food-insecure humans for Caputo derivative**

FIGURE 5. **Human Population**

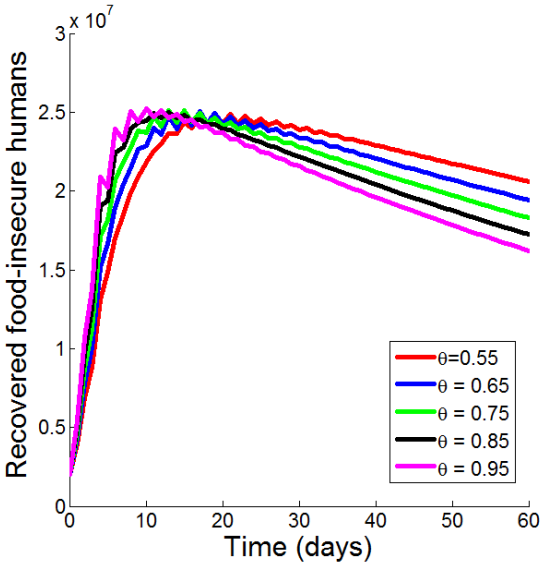

(A) **The plot for the recovered food-insecure humans for Caputo derivative**

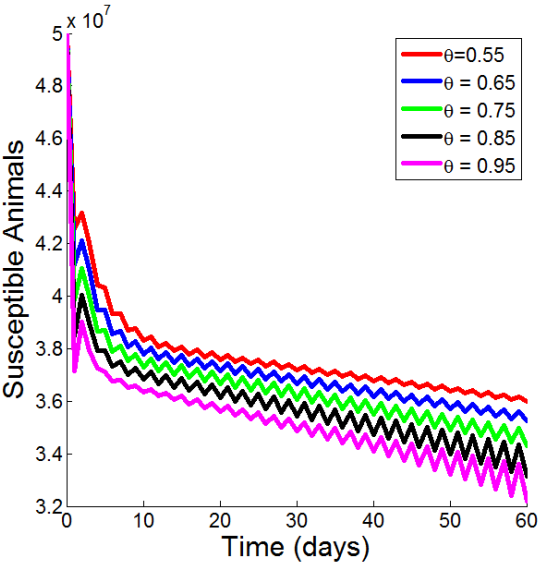

(B) **The plot for the Susceptible animals for Caputo derivative**

FIGURE 6. **Human and animal Population**

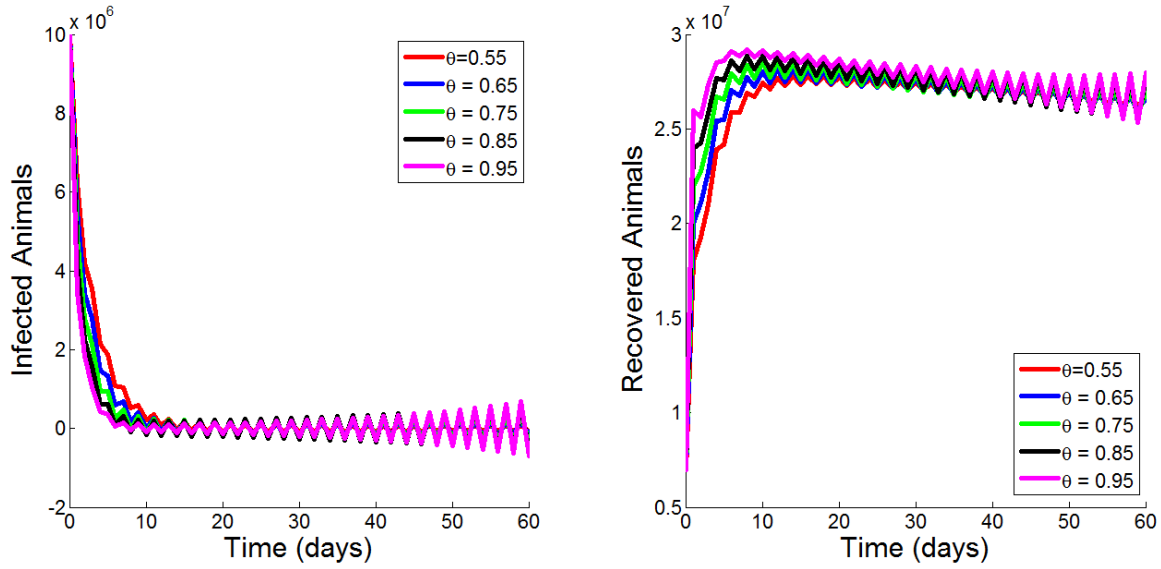

(A) **The plot for the Infected animals for Caputo derivative**

(B) **The plot for the Recovered animals for Caputo derivative**

FIGURE 7. **Animal Population**

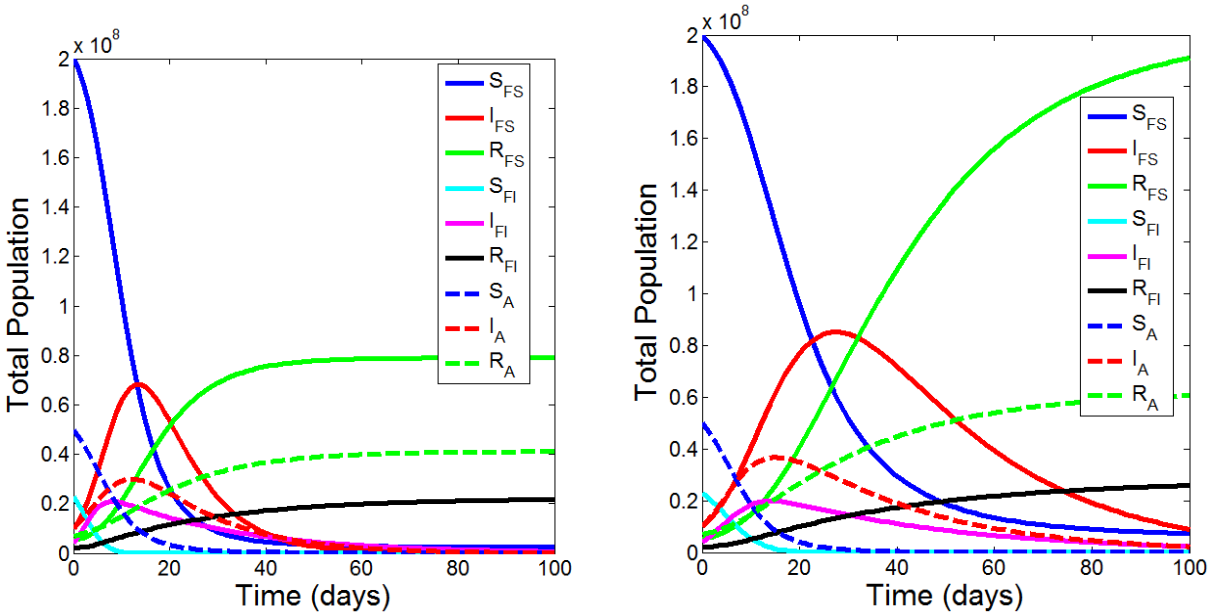

(A) **Behaviors of the system (10) by adopting Caputo-Fabrizio derivative for $\theta = 0.95$**

(B) **Behaviors of the system (10) by adopting Caputo-Fabrizio derivative for $\theta = 0.85$**

FIGURE 8. **Human Population**

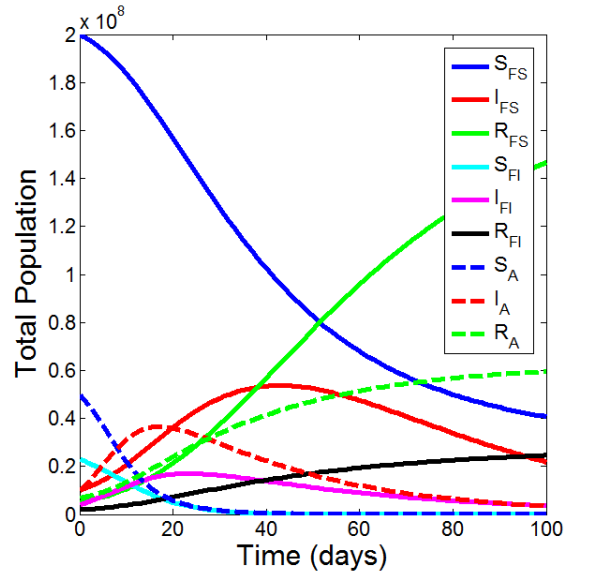

(A) **Behaviors of the system (10) by adopting Caputo-Fabrizio derivative for $\theta = 0.75$**

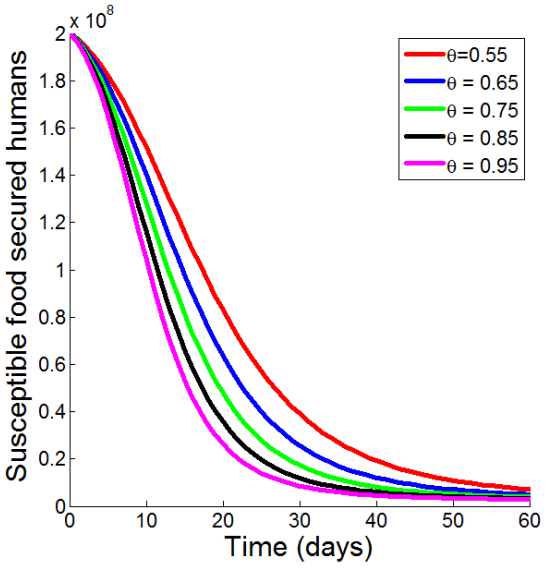

(B) **The plot for the susceptible food-secured population for Caputo Fabrizio derivative**

FIGURE 9. **Human Population**

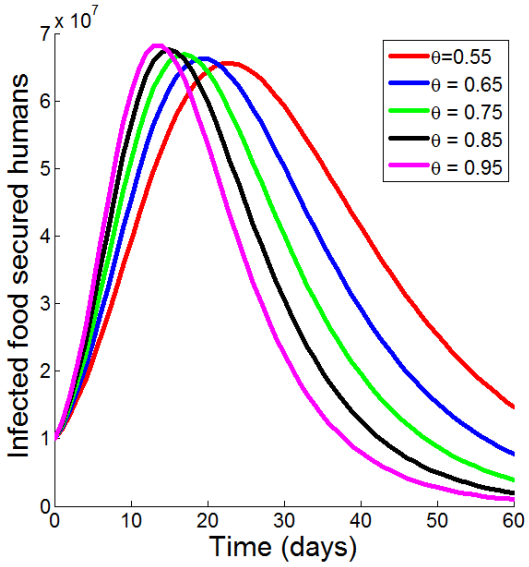

(A) **The plot for the infected food-secured population for Caputo Fabrizio derivative**

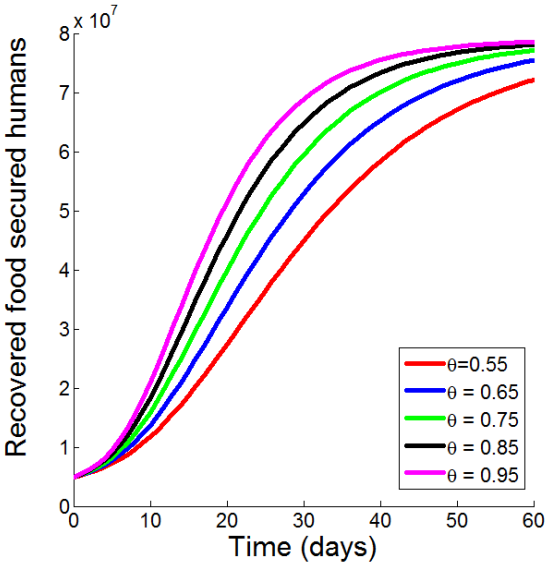

(B) **The plot for the recovered food-secured population for Caputo Fabrizio derivative**

FIGURE 10. **Human Population**

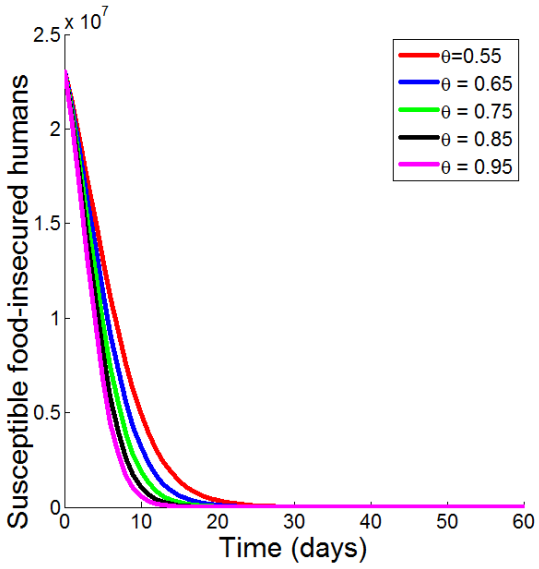

(A) **The plot for the susceptible food-insecure population for Caputo Fabrizio derivative**

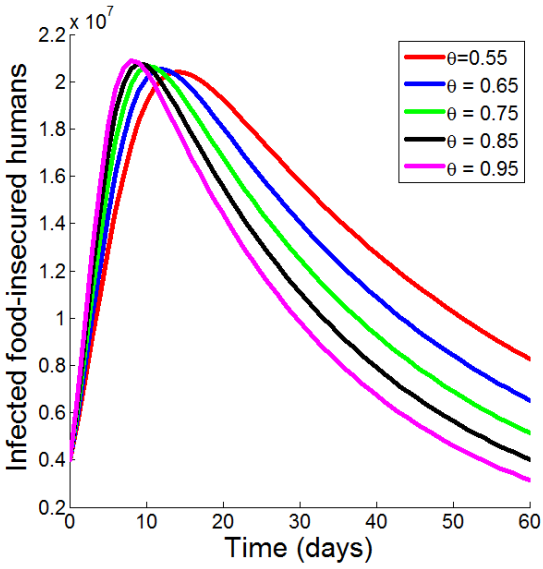

(B) **The plot for the infected food-insecure population for Caputo Fabrizio derivative**

FIGURE 11. **Human Population**

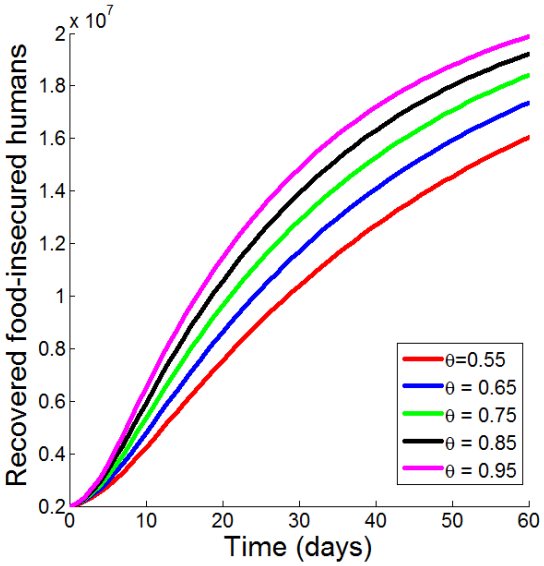

(A) **The plot for the recovered food-insecure population for Caputo Fabrizio derivative**

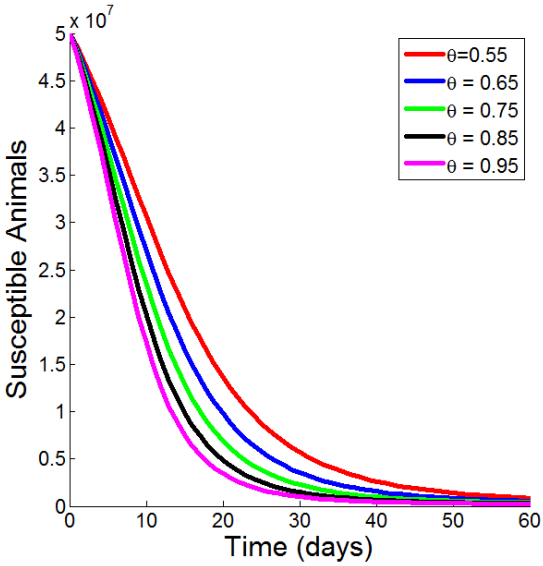

(B) **The plot for the susceptible animal population for Caputo Fabrizio derivative**

FIGURE 12. **Human and animal Population**

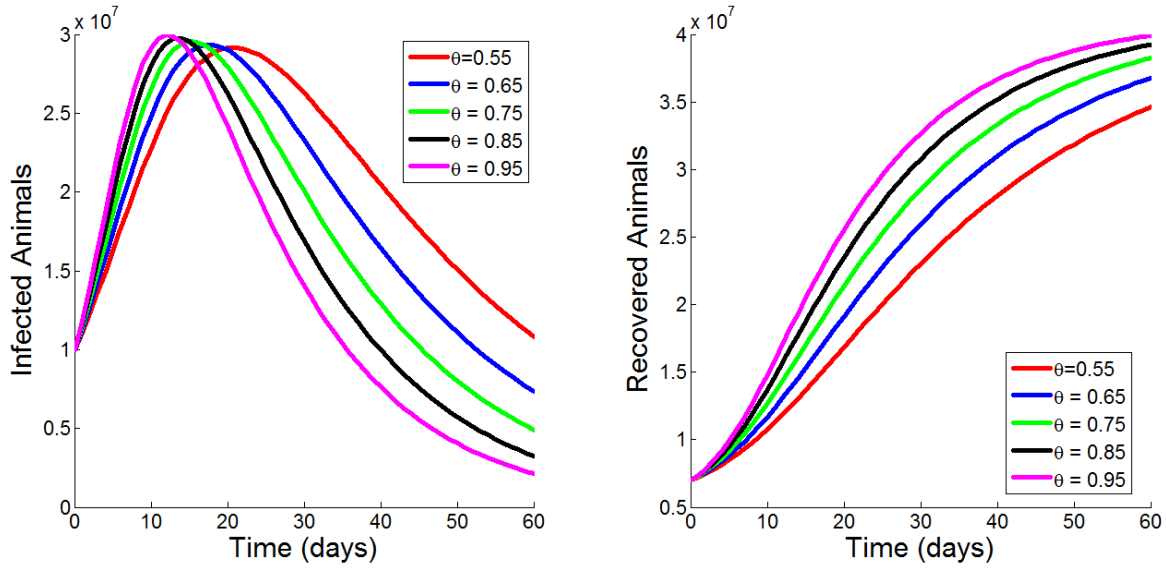

(A) **The plot for the infected animals for Caputo Fabrizio derivative**

(B) **The plot for the recovered animals for Caputo Fabrizio derivative**

FIGURE 13. **Animal Population**

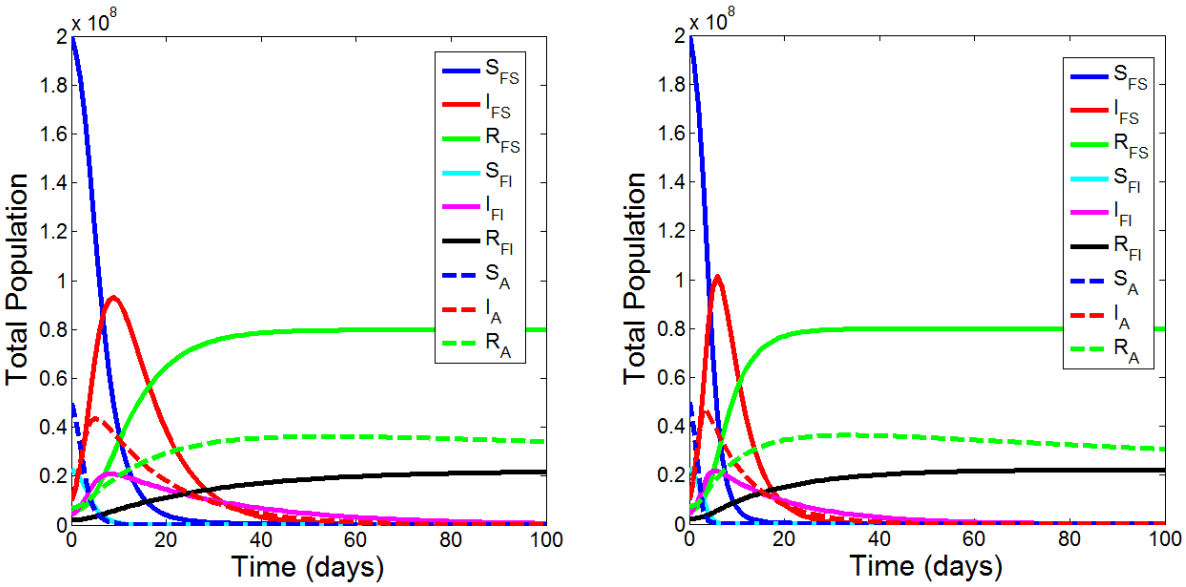

(A) **Behaviors of the system (11) by adopting Atagana Baleanu derivative for $\theta = 0.95$**

(B) **Behaviors of the system (11) by adopting Atagana Baleanu derivative for $\theta = 0.85$**

FIGURE 14. **Human Population**

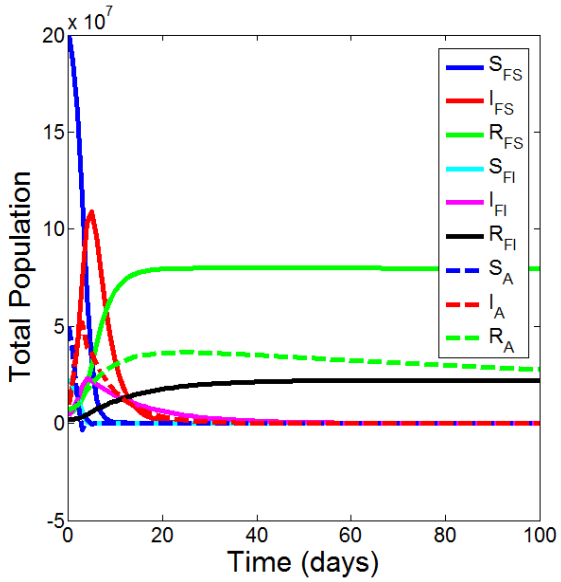

(A) **Behaviors of the system (11) by adopting Atagana Baleanu derivative for $\theta = 0.75$**

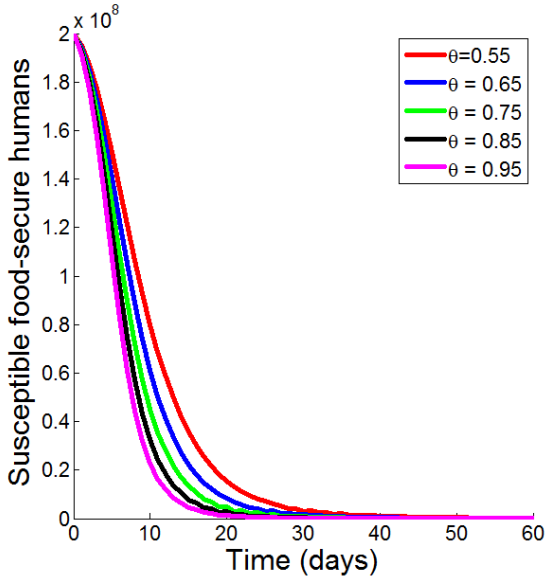

(B) **The plot for the susceptible food secure humans for Atagana Baleanu derivative**

FIGURE 15. **Human Population**

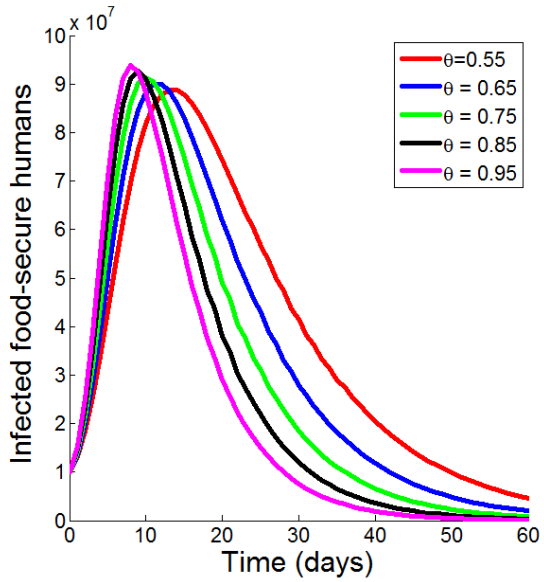

(A) **The plot for the infected food secure humans for Atagana Baleanu derivative**

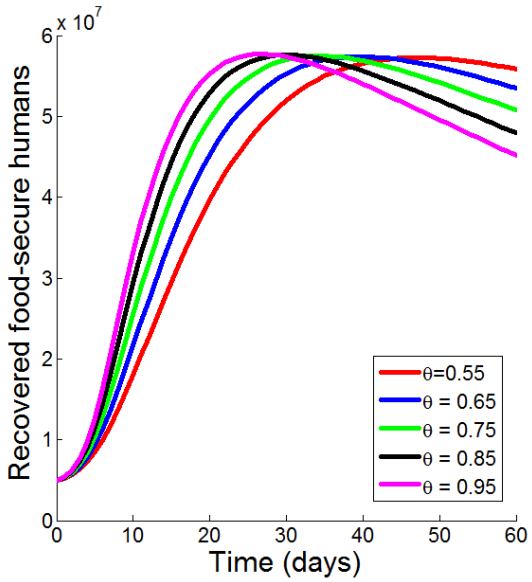

(B) **The plot for the recovered food secure humans for Atagana Baleanu derivative**

FIGURE 16. **Human Population**

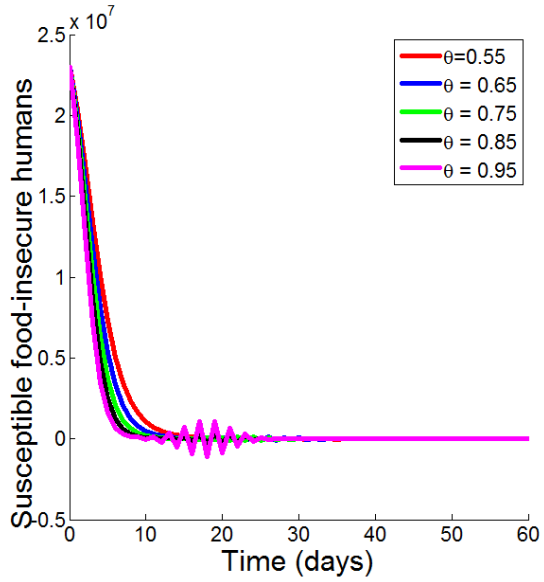

(A) **The plot for the susceptible food-insecure population for Atagana Baleanu derivative**

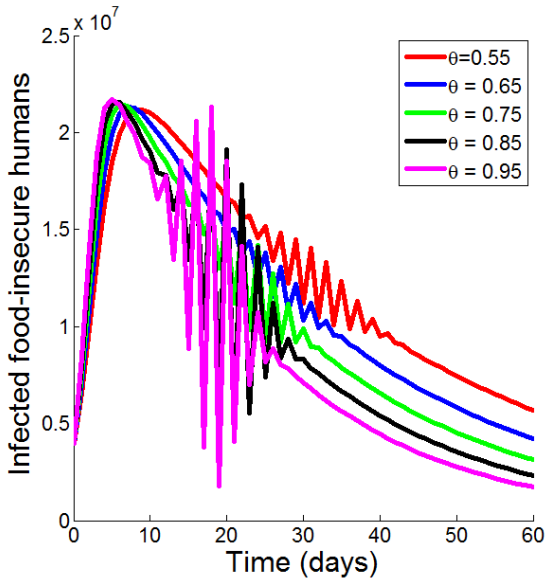

(B) **The plot for the infected food-insecure population for Atagana Baleanu derivative**

FIGURE 17. **Human Population**

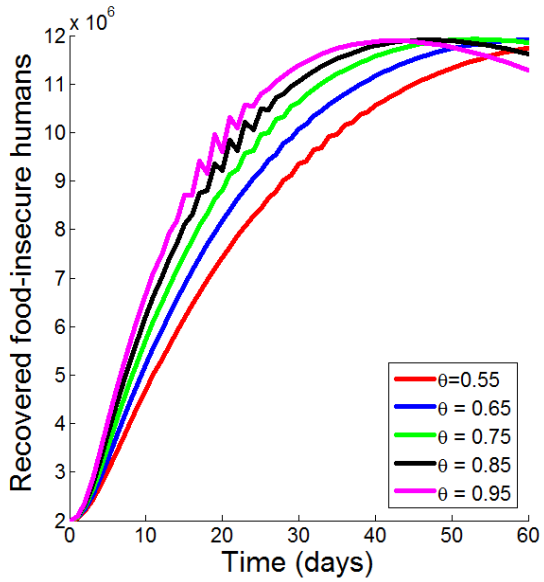

(A) **The plot for the recovered food-insecure population for Atagana Baleanu derivative**

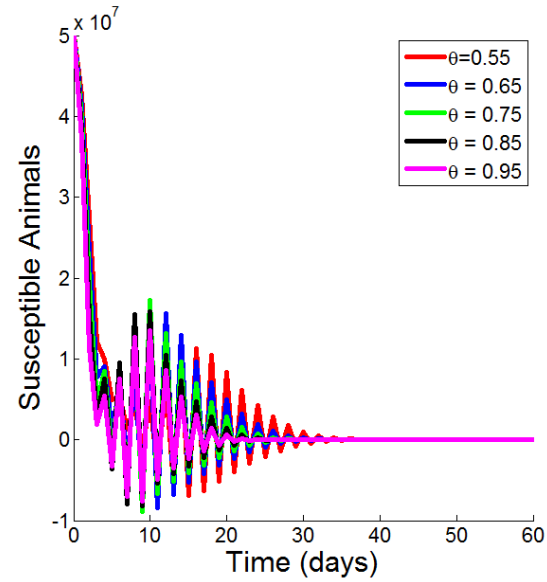

(B) **The plot for the susceptible animals for Atagana Baleanu derivative**

FIGURE 18. **Human and animal Population**

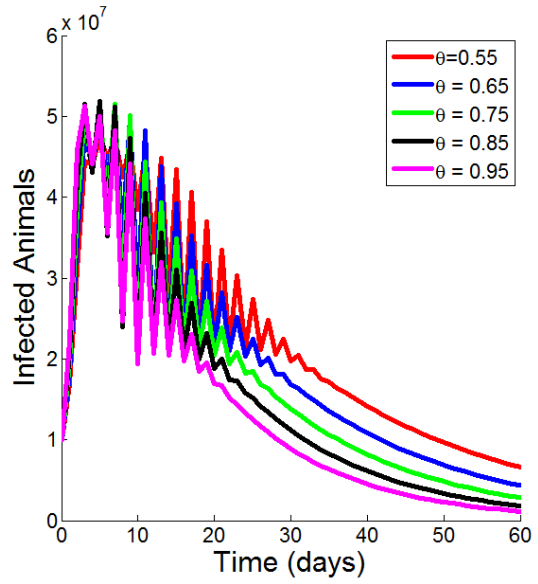

(A) **The plot for the infected animals for Atagana Baleanu derivative**

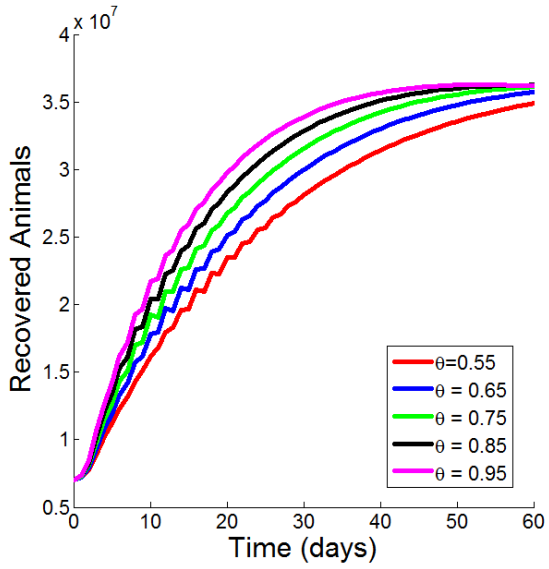

(B) **The plot for the recovered animals for Atagana Baleanu derivative**

FIGURE 19. **Animal Population**

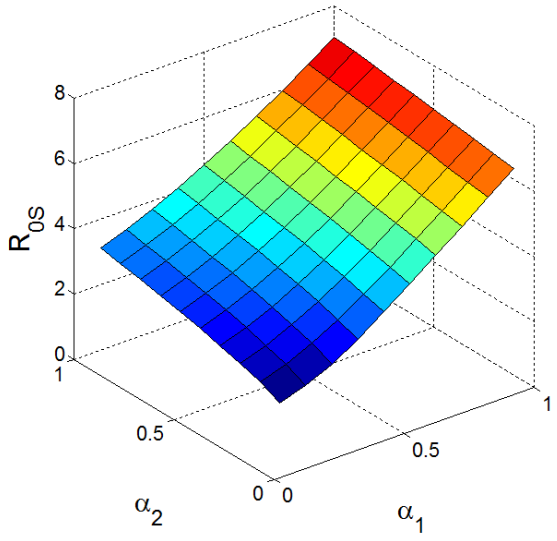

(A) **Surface plots of α_1 and α_2 against R_{0S}**

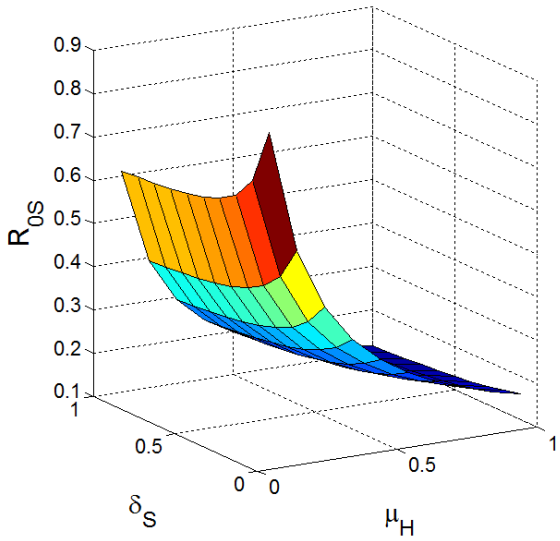

(B) **Surface plots of α_1 and α_2 against R_{0S}**

FIGURE 20. **Human Population**

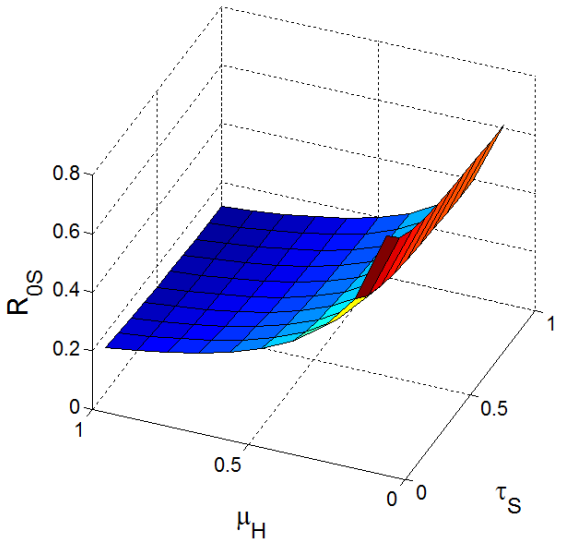

(A) **Surface plots of τ_S and μ_H against R_{0S}**

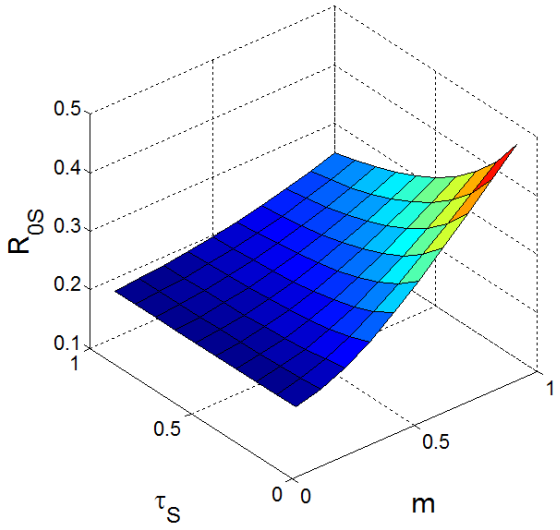

(B) **Surface plots of m and τ_S against R_{0S}**

FIGURE 21. **Human Population**

5. DISCUSSION

The graphs presented in Figures (2a, 2b, 3a) depict the dynamics of all compartments in the Monkeypox disease transmission model, governed by the system of equations in (6), under the Caputo fractional derivatives of orders 0.95, 0.85, and 0.75, respectively. These simulations provide significant insights into the effects of fractional-order dynamics on the spread of Monkeypox, with a particular focus on the role of food security in mitigating disease transmission. The application of Caputo fractional derivatives enables a detailed exploration of the temporal memory effects inherent in disease dynamics. As the fractional order increases, the population of susceptible humans demonstrates a notable decline, as illustrated in Figures (3b) and (5a). This decline can be attributed to the amplified effects of interventions, such as awareness campaigns and sensitization programs, which underscore the dangers associated with consuming unwholesome or improperly handled food, particularly meat. By reducing the likelihood of exposure to infectious agents, these interventions lead to a decrease in the number of susceptible individuals over time. The infected human populations, both in the food-secure and food-insecure groups, initially exhibit an increase due to the progression of individuals from the

susceptible compartment caused by the highly infectious nature of the disease. However, a subsequent decline is observed as individuals recover through treatment, immunity development, or other interventions. This trend is clearly illustrated in Figures (4a) and (5b). Interestingly, the peak number of infected cases in the food-secure population, approximately 9.5 million, is substantially lower than the 12.5 million cases observed in the food-insecure population. This stark contrast highlights the critical importance of food security in mitigating the transmission of Monkeypox.

Food security plays a vital role in reducing zoonotic transmission risks, achieved through practices such as proper food storage, ensuring hygiene, and minimizing contamination by infected animals. These practices significantly diminish the likelihood of animal-to-human transmission. On the other hand, food-insecure populations, characterized by limited access to hygienic food practices and insufficient awareness of associated risks, show higher susceptibility and infection rates. The findings underscore the need for targeted public health interventions in food-insecure regions to promote food safety practices and enhance disease awareness. The graphs in Figures (8) and (9) present the system dynamics under the Caputo-Fabrizio fractional derivative approach. For fractional orders $\theta = 0.95$, 0.85, and 0.75, this method reveals distinct behavioral characteristics of disease progression. The Caputo-Fabrizio derivative, characterized by its non-singular kernel, provides additional insights into the memory effects of disease transmission while allowing for smoother transitions between population states. The susceptible food-secure population exhibits a more gradual decline compared to the Caputo derivative approach, suggesting that the non-singular kernel better captures realistic behavioral responses to disease awareness. In Figures (14) through (19), the Atangana-Baleanu derivative analysis further enriches our understanding of disease dynamics. Incorporating the Mittag-Leffler function, this derivative captures unique long-term memory effects in disease transmission. The susceptible and infected populations demonstrate smoother transitions and more pronounced peaks compared to the Caputo and Caputo-Fabrizio approaches. This indicates that the Atangana-Baleanu derivative effectively represents scenarios where past events significantly influence current transmission rates. Surface plots in Figures (20) and (21) provide critical insights into

the sensitivity of the basic reproduction number, R_{0S}, to various model parameters. The plots reveal that higher contact rates (α_1, α_2) are associated with elevated R_{0S} values, indicating a faster spread of the disease. Similarly, the recovery rate (τ_S) and natural death rate (μ_H) are shown to influence the disease's propagation. The modification parameter m, reflecting food security status, demonstrates a significant role in altering transmission patterns. Lower values of m in food-secure populations correspond to reduced transmission rates, highlighting the protective impact of food security measures.

The dynamics of animal compartments, presented in Figures (6), (15), and (18), further emphasize the zoonotic nature of Monkeypox. These figures reveal how infected animal populations serve as reservoirs for the disease, maintaining its presence in human populations. Control strategies targeting both human and animal populations are essential to disrupt this transmission cycle effectively. The comprehensive analysis provided by the three fractional derivative approaches—Caputo, Caputo-Fabrizio, and Atangana-Baleanu—underscores the multifaceted dynamics of Monkeypox transmission. The results consistently demonstrate that food-insecure populations bear a disproportionate burden of the disease, characterized by higher infection peaks, slower recovery rates, and greater susceptibility to zoonotic transmission. This disparity necessitates integrated public health strategies combining traditional disease control measures with enhanced food security interventions. In conclusion, these mathematical analyses, coupled with visualizations, offer valuable insights into Monkeypox dynamics, emphasizing the critical role of food security and targeted interventions in disease mitigation. Improved food security emerges as a promising strategy for reducing the disease burden, particularly in vulnerable populations, thereby contributing to more effective and sustainable public health outcomes.

6. Conclusion

In order to comprehend the transmission dynamics of Monkeypox across populations with varying food security status, we evaluated a novel fractional-order mathematical model incorporating both human and animal compartments. The model was analyzed using three distinct fractional derivative operators: the Caputo derivative with power law, Caputo-Fabrizio with exponential law, and Atangana-Baleanu with generalized Mittag-Leffler function, making our analysis more comprehensive and robust. The numerical simulations reveal that increasing the

fractional order generally leads to a slower progression of the disease, reflecting the memory effects inherent in fractional derivatives. Specifically, higher values of the fractional order correspond to more gradual disease spread, as evidenced in the dynamics of both food-secure and food-insecure populations. This effect is particularly pronounced in the food-insecure population, where the peak infection rates reach approximately 12.5 million cases compared to 9.5 million in food-secure populations, highlighting the critical role of food security in disease transmission. Our results indicate that food security status significantly impacts the transmission dynamics of Monkeypox. The modification parameter (m) accounting for reduced disease contraction in food-secure populations demonstrates that improved food security measures lead to a notable decrease in cumulative cases. This is attributed to better food handling practices, reduced exposure to infected animals, and improved access to healthcare resources in food-secure populations. The model shows that higher rates of recovery (τ_S, τ_I) and lower contact rates ($\alpha_1, \alpha_2, \alpha_3$) in food-secure populations result in lower peaks of infections and faster decline in new cases, emphasizing the importance of food security interventions in disease control. The surface plots analyzing the basic reproduction number R_0^S against various parameters reveal critical thresholds for disease control, particularly highlighting the relationship between food security status and transmission rates. These findings underscore the necessity of implementing comprehensive public health strategies that address both direct disease transmission and underlying socioeconomic factors, especially food security. In summary, the arbitrary-order derivative operators applied in this study provide enhanced understanding of the complex dynamics of Monkeypox transmission. The model successfully captures the crucial role of food security in disease progression and suggests that integrated approaches combining traditional disease control measures with food security interventions may be most effective in controlling Monkeypox outbreaks, particularly in vulnerable populations.

CONFLICT OF INTERESTS

The authors declare that there is no conflict of interests.

REFERENCES

[1] O.C. Collins, K.J. Duffy, Dynamics and Control of Mpox Disease Using Two Modelling Approaches, Model. Earth Syst. Environ. 10 (2024), 1657–1669. https://doi.org/10.1007/s40808-023-01862-8.

[2] E.M. Bunge, B. Hoet, L. Chen, F. Lienert, H. Weidenthaler, L.R. Baer, R. Steffen, The Changing Epidemiology of Human Monkeypox—A Potential Threat? A Systematic Review, PLOS Neglected Trop. Dis. 16 (2022), e0010141. https://doi.org/10.1371/journal.pntd.0010141.

[3] S. Usman, I. Isa Adamu, Modeling the Transmission Dynamics of the Monkeypox Virus Infection with Treatment and Vaccination Interventions, J. Appl. Math. Phys. 05 (2017), 2335–2353. https://doi.org/10.4236/jamp.2017.512191.

[4] CDC, Signs and Symptoms of Mpox, (2023). https://www.cdc.gov/mpox/signs-symptoms/?CDC_AAref_Val=https://www.cdc.gov/poxvirus/mpox/symptoms/index.html.

[5] E. Alakunle, U. Moens, G. Nchinda, M.I. Okeke, Monkeypox Virus in Nigeria: Infection Biology, Epidemiology, and Evolution, Viruses 12 (2020), 1257. https://doi.org/10.3390/v12111257.

[6] D.B. Di Giulio, P.B. Eckburg, Human Monkeypox: An Emerging Zoonosis, Lancet Infect. Dis. 4 (2004), 15–25. https://doi.org/10.1016/S1473-3099(03)00856-9.

[7] U.E. Michael, L.O. Omenyi, E. Kafayat, et al. Monkeypox Mathematical Model With Surveillance as Control, Commun. Math. Biol. Neurosci. 2023 (2023), 6. https://doi.org/10.28919/cmbn/7781.

[8] M.S. Maldonado, A.J. Lucchetti, R.A.P. Pacheco, et al. Epidemiologic Characteristics and Clinical Features of Patients with Monkeypox Virus Infection from a Hospital in Peru between July and September 2022, Int. J. Infect. Dis. 129 (2023), 175–180. https://doi.org/10.1016/j.ijid.2023.01.045.

[9] M.W. McCarthy, Therapeutic Strategies to Address Monkeypox, Expert Rev. Anti-Infect. Ther. 20 (2022), 1249–1252. https://doi.org/10.1080/14787210.2022.2113058.

[10] J.P. Thornhill, S. Barkati, S. Walmsley, et al. Monkeypox Virus Infection in Humans across 16 Countries — April–June 2022, N. Engl. J. Med. 387 (2022), 679–691. https://doi.org/10.1056/NEJMoa2207323.

[11] B. Ortiz-Saavedra, D.A. León-Figueroa, E.S. Montes-Madariaga, et al. Antiviral Treatment against Monkeypox: A Scoping Review, Trop. Med. Infect. Dis. 7 (2022), 369. https://doi.org/10.3390/tropicalmed7110369.

[12] Centers for Disease Control and Prevention, 2022-2023 Mpox Outbreak Global Map. https://archive.cdc.gov/www_cdc_gov/poxvirus/mpox/response/2022/world-map.html.

[13] World Health Organization, Monkeypox Outbreak, (2024). https://www.who.int/emergencies/situations/mpox-outbreak.

[14] J.B. Nuzzo, L.L. Borio, L.O. Gostin, The WHO Declaration of Monkeypox as a Global Public Health Emergency, JAMA 328 (2022), 615. https://doi.org/10.1001/jama.2022.12513.

[15] Centers for Disease Control and Prevention, Ongoing Clade II Mpox Global Outbreak, (2023). https://www.cdc.gov/mpox/outbreaks/2022/index-1.html.

[16] P.F. Adebayo, E.O. Ojo, Food Security in Nigeria: An Overview, Eur. J. Sustain. Dev. 1 (2012), 199–222. https://doi.org/10.14207/ejsd.2012.v1n2p199.

[17] World Food Programme, Food Security – What It Means and Why It Matters, (2025). https://www.wfp.org/stories/food-security-what-it-means-and-why-it-matters.

[18] N. Ahmad, S.K. Shahnawaz, Z. Alam, Food Insecurity: Concept, Causes, Effects and Possible Solutions, IAR J. Human. Soc. Sci. 2.1 (2021), 105–113.

[19] W.O. Fawole, E. Ilbasmis, B. Ozkan, Food Insecurity in Africa in Terms of Causes, Effects, and Solutions: A Case Study of Nigeria, in: 2nd International Conference on Sustainable Agriculture and Environment (ICSAE 2015), (2015), 1–9.

[20] R.L. Magin, Fractional Calculus Models of Complex Dynamics in Biological Tissues, Comput. Math. Appl. 59 (2010), 1586–1593. https://doi.org/10.1016/j.camwa.2009.08.039.

[21] K. Hattaf, Z. Hajhouji, M. Ait Ichou, N. Yousfi, A Numerical Method for Fractional Differential Equations with New Generalized Hattaf Fractional Derivative, Math. Probl. Eng. 2022 (2022), 3358071. https://doi.org/10.1155/2022/3358071.

[22] B. Ghanbari, On Novel Nondifferentiable Exact Solutions to Local Fractional Gardner's Equation Using an Effective Technique, Math. Methods Appl. Sci. 44 (2021), 4673–4685. https://doi.org/10.1002/mma.7060.

[23] B.B. Mandelbrot, J.W. Van Ness, Fractional Brownian Motions, Fractional Noises and Applications, SIAM Rev. 10 (1968), 422–437. https://doi.org/10.1137/1010093.

[24] A. Ali, S. Das, Applications of Neuro-Computing and Fractional Calculus to Blood Streaming Conveying Modified Trihybrid Nanoparticles with Interfacial Nanolayer Aspect inside a Diseased Ciliated Artery under Electroosmotic and Lorentz Forces, Int. Commun. Heat Mass Transfer 152 (2024), 107313. https://doi.org/10.1016/j.icheatmasstransfer.2024.107313.

[25] P.A. Naik, M. Farman, A. Zehra, K.S. Nisar, E. Hincal, Analysis and Modeling with Fractal-Fractional Operator for an Epidemic Model with Reference to COVID-19 Modeling, Partial Differ. Equ. Appl. Math. 10 (2024), 100663. https://doi.org/10.1016/j.padiff.2024.100663.

[26] I. Podlubny, Fractional Differential Equations: An Introduction to Fractional Derivatives, Fractional Differential Equations, to Methods of Their Solution and Some of Their Applications, Academic Press, San Diego, 1999.

[27] P. Kórus, J.E. Nápoles Valdés, Recent Advances in Fractional Calculus, Axioms 13 (2024), 310. https://doi.org/10.3390/axioms13050310.

[28] J.E. Macías-Díaz, Fractional Calculus—Theory and Applications, Axioms 11 (2022), 43. https://doi.org/10.3390/axioms11020043.

[29] S. Okyere, J. Ackora-Prah, Modeling and Analysis of Monkeypox Disease Using Fractional Derivatives, Results Eng. 17 (2023), 100786. https://doi.org/10.1016/j.rineng.2022.100786.

[30] G.O. Acheneje, D. Omale, B.C. Agbata, W. Atokolo, M.M. Shior, B. Bolarinwa, Approximate Solution of the Fractional Order Mathematical Model on the Transmission Dynamics on The Co-Infection of COVID-19 and Monkeypox Using the Laplace-Adomian Decomposition Method, Int. J. Math. Stat. Stud. 12 (2024), 17–51. https://doi.org/10.37745/ijmss.13/vol12n31751.

[31] M.A. Qurashi, S. Rashid, A.M. Alshehri, F. Jarad, F. Safdar, New Numerical Dynamics of the Fractional Monkeypox Virus Model Transmission Pertaining to Nonsingular Kernels, Math. Biosci. Eng. 20 (2022), 402–436. https://doi.org/10.3934/mbe.2023019.

[32] A. Atangana, D. Baleanu, New Fractional Derivatives with Nonlocal and Non-Singular Kernel: Theory and Application to Heat Transfer Model, Therm. Sci. 20 (2016), 763–769. https://doi.org/10.2298/TSCI160111018A.

[33] M. Caputo, M. Fabrizio, A New Definition of Fractional Derivative Without Singular Kernel, Progr. Fract. Differ. Appl. 1 (2015), 73–85.

[34] A. Atangana, K.M. Owolabi, New Numerical Approach for Fractional Differential Equations, Math. Model. Nat. Phenom. 13 (2018), 3. https://doi.org/10.1051/mmnp/2018010.

[35] K. Logeswari, C. Ravichandran, A New Exploration on Existence of Fractional Neutral Integro-Differential Equations in the Concept of Atangana-baleanu Derivative, Physica A: Stat. Mech. Appl. 544 (2020) 123454. https://doi.org/10.1016/j.physa.2019.123454.

[36] S.K. Panda, T. Abdeljawad, C. Ravichandran, A Complex Valued Approach to the Solutions of Riemann-Liouville Integral, Atangana-Baleanu Integral Operator and Non-Linear Telegraph Equation via Fixed Point Method, Chaos Solitons Fractals 130 (2020), 109439. https://doi.org/10.1016/j.chaos.2019.109439.

[37] S.K. Panda, T. Abdeljawad, C. Ravichandran, Novel Fixed Point Approach to Atangana-Baleanu Fractional and Lp-Fredholm Integral Equations, Alexandria Eng. J. 59 (2020), 1959–1970. https://doi.org/10.1016/j.aej.2019.12.027.

[38] C. Ravichandran, K. Logeswari, F. Jarad, New Results on Existence in the Framework of Atangana–baleanu Derivative for Fractional Integro-Differential Equations, Chaos Solitons Fractals 125 (2019), 194–200. https://doi.org/10.1016/j.chaos.2019.05.014.

[39] C. Ravichandran, K. Logeswari, S.K. Panda, K.S. Nisar, On New Approach of Fractional Derivative by Mittag-Leffler Kernel to Neutral Integro-Differential Systems With Impulsive Conditions, Chaos Solitons Fractals 139 (2020), 110012. https://doi.org/10.1016/j.chaos.2020.110012.

[40] N. Valliammal, C. Ravichandran, K.S. Nisar, Solutions to Fractional Neutral Delay Differential Nonlocal Systems, Chaos Solitons Fractals 138 (2020), 109912. https://doi.org/10.1016/j.chaos.2020.109912.

[41] J. Losada, J.J. Nieto, Properties of a New Fractional Derivative Without Singular Kernel, Progr. Fract. Differ. Appl. 1 (2015), 87–92.

[42] B.S.T. Alkahtani, A. Atangana, I. Koca, Novel Analysis of the Fractional Zika Model Using the Adams Type Predictor-Corrector Rule for Non-Singular and Non-Local Fractional Operators, J. Nonlinear Sci. Appl. 10 (2017), 3191–3200. https://doi.org/10.22436/jnsa.010.06.32.

[43] worldometers, Nigeria Population (2024). https://www.worldometers.info/world-population/nigeria-population.

[44] G.O. Acheneje, D. Omale, W. Atokolo, B. Bolaji, Modeling the Transmission Dynamics of the Co-Infection of Covid-19 and Monkeypox Diseases With Optimal Control Strategies and Cost–benefit Analysis, Franklin Open 8 (2024), 100130. https://doi.org/10.1016/j.fraope.2024.100130.

[45] C.P. Bhunu, W. Garira, G. Magombedze, Mathematical Analysis of a Two Strain HIV/AIDS Model with Antiretroviral Treatment, Acta Biotheor. 57 (2009), 361–381. https://doi.org/10.1007/s10441-009-9080-2.

[46] M.R. Odom, R. Curtis Hendrickson, E.J. Lefkowitz, Poxvirus Protein Evolution: Family Wide Assessment of Possible Horizontal Gene Transfer Events, Virus Res. 144 (2009), 233–249. https://doi.org/10.1016/j.virusres.2009.05.006.

[47] O.J. Peter, S. Kumar, N. Kumari, et al. Transmission Dynamics of Monkeypox Virus: A Mathematical Modelling Approach, Model. Earth Syst. Environ. 8 (2021), 3423–3434. https://doi.org/10.1007/s40808-021-01313-2.